NPS-59Nn75061A

NAVAL POSTGRADUATE SCHOOL

Monterey, California

DYNAMICS OF LIQUID PROPELLANT
GUN LOADING SYSTEMS
Annual Progress Report

by

R. H. Nunn
E. J. Gibson

1 June 1975

NAVAL POSTGRADUATE SCHOOL
Monterey, California

Rear Admiral Isham Linder
Superintendent

J. R. Borsting
Provost

DYNAMICS OF LIQUID PROPELLANT GUN LOADING SYSTEMS

This report documents the progress during FY75 in the analytical and experimental investigation of the behavior of a liquid propellant during loading into the breech of a liquid propellant gun. A one-dimensional model was constructed for the unsteady behavior of the assumed incompressible liquid. An experimental loading system was designed and fabricated to test the model and to identify critical design constraints. The analytical model, supported by the experiments, was utilized to conduct parametric studies and to provide guidance to designers of liquid propellant gun loading systems.

The work reported herein has been monitored and supported by the Naval Ordnance Station, Indian Head, and the project was initiated by the Naval Surface Weapons Center, Dahlgren, by means of Project Order No. PO 4-006B.

SECURITY CLASSIFICATION OF THIS PAGE *(When Data Entered)*

REPORT DOCUMENTATION PAGE

READ INSTRUCTIONS BEFORE COMPLETING FORM

1. REPORT NUMBER: NPS-59Nn75061A	2. GOVT ACCESSION NO.
3. RECIPIENT'S CATALOG NUMBER	
4. TITLE *(and Subtitle)*: DYNAMICS OF LIQUID PROPELLANT GUN LOADING SYSTEMS	5. TYPE OF REPORT & PERIOD COVERED: Annual Progress, FY75
6. PERFORMING ORG. REPORT NUMBER	
7. AUTHOR*(s)*: R. H. Nunn E. J. Gibson	8. CONTRACT OR GRANT NUMBER*(s)*
9. PERFORMING ORGANIZATION NAME AND ADDRESS: Naval Postgraduate School Monterey, California 93940	10. PROGRAM ELEMENT, PROJECT, TASK AREA & WORK UNIT NUMBERS: PO 4-006B
11. CONTROLLING OFFICE NAME AND ADDRESS: Code 5032E Naval Ordnance Station Indianhead, MD	12. REPORT DATE: 1 June 75
	13. NUMBER OF PAGES
14. MONITORING AGENCY NAME & ADDRESS*(if different from Controlling Office)*	15. SECURITY CLASS. *(of this report)*: Unclassified
	15a. DECLASSIFICATION/DOWNGRADING SCHEDULE

16. DISTRIBUTION STATEMENT *(of this Report)*

Approved for public release; distribution unlimited.

17. DISTRIBUTION STATEMENT *(of the abstract entered in Block 20, if different from Report)*

18. SUPPLEMENTARY NOTES

19. KEY WORDS *(Continue on reverse side if necessary and identify by block number)*

Liquid Propellant Gun, Fluid Dynamics, Loading, Handling Control

20. ABSTRACT *(Continue on reverse side if necessary and identify by block number)* This report documents the progress during FY75 in the analytical and experimental investigation of the behavior of a liquid propellant during loading into the breech of a liquid propellant. A one-dimensional model was constructed for the unsteady behavior of the assumed incompressible liquid. An experimental loading system was designed and fabricated to test the model and to identify critical design constraints. The analytical model supported by the experiments, was utilized to conduct parametric studies and to provide guidance to designers of liquid propellant gun loading systems.

DD FORM 1 JAN 73 1473 EDITION OF 1 NOV 65 IS OBSOLETE
S/N 0102-014-6601 |

SECURITY CLASSIFICATION OF THIS PAGE *(When Data Entered)*

TABLE OF CONTENTS

DYNAMICS OF LIQUID PROPELLANT GUN LOADING SYSTEMS

Annual Progress Report, FY75

I. INTRODUCTION AND BACKGROUND

A. LIQUID PROPELLANTS FOR ADVANCED NAVY GUN SYSTEMS

With continued trends toward more sophisticated weapons platforms to meet the projected threats of a hostile environment, improved gun systems will be required. These systems of the future will have to have a total weight less than existing gun systems of the same caliber, a less complicated logistics train, improved capabilities, and they will have to be cost effective. Various analytical and experimental investigations conducted over a period of approximately thirty years have demonstrated that the potential advantages of liquid propellant guns (LPG's) are sufficient to warrant their serious consideration as candidate elements in advanced naval gun systems.

The following remarks are intended to illustrate some of these potential advantages. By eliminating the cartridge case, both airborne and surface platforms will be able to carry more shots per pound and/or a more varied assortment of weapons. At the present time, shipboard guns using semi-fixed ammunition require a separate magazine for powder in relatively close proximity to the gun. By

using a liquid propellant, the propellant tanks could be located anywhere in the ship without great difficulty, thus allowing the ship designer more flexibility. With a standardized propellant, different caliber guns, which now use both semi-fixed and fixed ammunition, could be supplied from the same tank, eliminating the separate spaces needed to conform with ordnance storage compatibility requirements. Redistribution of propellants onboard could be accomplished by means of pumping rather than manual labor or an elaborate mechanical transfer system. Propellant retrograde materials, e.g., pallets, powder cases, and powder cans, would be eliminated. Underway replenishment and rearming evolutions would consist of taking on projectiles and liquid, thus significantly reducing time, cost, and effort. Ship stability might be improved by the elimination of propellant weight in ready-service spaces. A ship sustaining battle damage could easily improve her stability by redistributing propellant or pumping it over the side. Increased firing rates may be attainable. It is because of this prospectus and improved technology in the field of monopropellants and bipropellants for gun applications that a research and development effort has again been initiated in the liquid propellant gun (LPG) area of ordnance development.

B. REVIEW OF PREVIOUS DEVELOPMENTS

In order to establish a point of departure for current developmental efforts in LPG technology, it is useful to briefly review the experiences documented by previous investigators. A review of LPG history was conducted, but the following remarks refer only to unclassified literature.

Interest in LPG systems in the United States was evident as early as 1945 [1] when the Army Office of the Chief of Ordnance conducted some preliminary calculations of the performance expected from liquid propellants. It was concluded that artillery performance could be greatly improved by using liquid propellants instead of solid propellants. Initial experimental investigation was in the area of bipropellants and feasibility demonstrations were conducted with a smooth bore, caliber .50 gun. These early tests resulted in surprisingly high muzzle velocities which seemed to spur increasing interest. It was discovered that to inject the propellant properly, an injection pressure in excess of chamber pressure was required [1]. To circumvent this problem, pre-loaded cased rounds were used. Large variations in the ballistic behavior without repeatability were noted [2].

In 1948, investigation into the feasibility of regenerative injection of bipropellants was begun [3]. The regenerative injection technique utilizes a differential area piston to extract energy from the burning propellant to power the injection process. It was determined that regenerative injection was feasible. However, continued study through 1950 with caliber .50 guns emphasized the need for high pressure static and dynamic seal improvement. It was also noted that lower mixing intensities gave lower muzzle velocities and excessive round-to-round variations were encountered with dilute bipropellants [4]. On the positive side, liquid propellants produced less bore wear than the existing solid propellants.

Concurrently, work was started on a 37-mm gun, based on the caliber .50 work [5, 6]. The 37-mm gun had regenerative injection with

nitrogen pressure to start the process. Feasibility of using the regenerative process in 37mm guns was proven; however, further development in the area of seals was again indicated.

The Navy became interested and began investigation of LPG systems in 1949 with an emphasis on improved performance for aircraft guns [7, 8]. Larger guns with higher velocities at the same size and weight were also desired. Naval Ammunition Depot, Seal Beach, California, started research and development of a 40mm monopropellant gun. The monopropellant developed seemed to satisfy all of the desired propellant criteria, however, for their initial gun tests, a bipropellant was used in a pre-loaded casing. At the same time, separate research was being done in the area of propellants themselves [9].

It should be noted that, as of 1950, the majority of the interest in liquid propellant guns was in the Army. They were mainly interested in LPG technology vice development, with a major interest in the end application to antiaircraft weapons. The high muzzle velocities and high rates of fire anticipated could readily satisfy the requirements for this role. Another use contemplated for LPG's was aircraft machine guns, because of the high rates of fire and the elimination of cartridge cases.

With the commencement of hostilities in Korea, the Army's LPG interest shifted to the area of infantry and tank weapons. The hypervelocities and greatly increased number of rounds per reload were extremely desirable characteristics for infantry weapons. A program specifically designed to employ liquid propellants in an existing 90mm gun as a tank weapon was started in 1950 [10]. This retrofit

program was aimed at improving the armor penetration of Army guns in Korea. The concept was to fit into a standard cartridge case the components of a hypergolic bipropellant system necessary to achieve muzzle velocities in excess of a standard round. Hypergolic bipropellants are designed to ignite spontaneously upon mixing. For a liquid propellant gun, this implies that no initiator is needed for ignition. These hypergolic bipropellants require an injection or mixing process. In the event of accidental contact of fuel and oxidizer, a fire would inevitably occur. Separate fuel and oxidizer containers were placed in the cartridge case with a mechanism to effect mixing. After two years of work, the design objectives had not been reached; only a half charge of propellant could be used without over-pressurizing the gun.

Actual small-caliber design studies of caseless guns were started in the early 1950's. The major emphasis in this field was on aircraft machine guns. A caliber .60 gun was designed in 1953 incorporating a regenerative injector monopiston to introduce both fuel and oxidizer in equal amounts into the chamber [11]. The design rate of fire was 2,000 rounds per minutes. However, the projectile and propellant feed systems interacted in such a way that projectile feed could inhibit propellant loading. It was recommended that a revolver type feed system be investigated. The reproducibility of ballistic characteristics, misfire procedures, overpressurization of the gun, propellant ignition, and ullage problems continually plagued these early efforts in liquid propellant gun research.

Until 1955, LPG systems consisted primarily of two general classes, preloaded and injection guns. Bipropellants and monopropellants have

been employed in each system with varying degrees of success. Preloaded guns, though simple in design, were extremely sensitive to loading density and ignition variations. Injection guns, though relatively complex, offered a positive means of combustion control. In an attempt to utilize the advantages of the various systems previously investigated, a project was started in 1955 to combine the two systems into a single monopropellant system approaching the simplicity of a preloaded gun, yet having the advantage of combustion control through injection [12]. A 40mm model was designed, featuring regenerative injection. A low-pressure static, high-pressure dynamic seal configuration was adopted to circumvent earlier problems encountered. Marginal performance was obtained with the system.

At the same time, the Navy funded research in the area of monopropellant and bipropellant injector systems for a 30mm gun for aircraft applications. This design incorporated a breech bleed feature to reduce ullage.

A 40mm development program was started as a prototype for a 3 to 5 inch rapid fire gun [13]. The 40mm was selected for testing purposes as a caseless gun. This effort was apparently terminated after the gun was damaged.

A number of projects were in progress in the mid-50's which were aimed at producing a 90mm tank gun [14, 15, 16, 17]. These programs continued to strive for hypervelocities by employing regeneratively injected bipropellants. An impressive increase in gun-tube life was anticipated; however, the injection system was somewhat large for tank application. At this point (1957), development aimed at major-caliber end items for Army use appears to have stopped, although some small-arms

studies continued. Among the reasons for this curtailment of research would appear to be the movement to a peace-time economy with the cessation of hostilities in Korea and the growth of missile technology.

In 1968, programs were started by the Navy which addressed the development of a safer aircraft machine gun with improved performance [18]. The use of non-hypergolic, preloaded, caseless liquid bipropellants was the course of action selected. After encouraging initial results, the program was continued with emphasis placed on developing a 20mm burst-fire gun. These programs utilized red fuming nitric acid (RFNA) as a propellant ingredient. One of these programs investigated a rotating four-barreled, cam operated system designed for a rate of fire of 1000 rounds per minute. It employed a pressurized injector feed system having an injection period of 11.3 milliseconds [19]. A computer simulation indicated the system would perform satisfactorily; however, a working model was not constructed. A similar program conducted simultaneously also employed a multi-barreled design [20]. A single barrel test gun was manufactured and fired in single shot tests. In the multi-barreled design, the projectile would be seated by propellant pressure. A nitrogen pressurized accumulator system for the propellant was employed to maintain propellant pressure. For the inert tests, water was used as the propellant simulator.

C. SCOPE AND OBJECTIVES OF THE PRESENT STUDY

The overall goal of this investigation is to both analytically and experimentally simulate and study the behavior of a liquid under conditions analogous to those existing in a rapid-fire LPG feed system.

The results of the study are intended to be useful in the identification of upper and lower bounds for such LPG design and performance parameters as time-to-load, injection supply pressure, injection system configuration (line lengths, diameters, accelerating masses, and viscous and minor losses), ullage, charge-to-mass ratio, caliber size, and projectile mass. In addition, the investigation has been designed to detect and characterize "anomalous" behaviors such as chamber pressure oscillations during loading, existence and consequences of cavitation in the liquid slug, and various sources of delay in the loading system. It has been felt that laboratory observation of effects such as these will prove to be essential in understanding the behavior of LPG prototype systems and future operational devices.

D. APPROACH AND PROGRESS

The investigation has taken the classical approach of analysis complemented by experimental tests. The analytical model has been constructed with a view towards simplicity while maintaining flexibility to refine the analysis as required to meet design requirements and to incorporate new information as LPG technology advances. The analytical model in its current form assumes one-dimensional unsteady flow of an incompressible propellant. This latter assumption is viewed as the most critical deficiency in the analysis and is a recommended area for follow-on efforts. It will be seen, however, that the analytical model in its present form is adequate for use in obtaining preliminary design guidance.

The experimental portion of the study has been primarily designed to support and validate (hopefully) the analytical model. Accordingly,

no special effort has been made to emulate existing or envisioned LPG designs. Off-the-shelf hardware has been used in the construction of the laboratory LPG simulator so that the performance of the device is somewhat less than might be obtained from an optimally designed system. The analytical model accurately predicts this "off-design" performance and points the way toward the areas of redesign that are likely to be most beneficial. This redesign is another area recommended for the expenditure of future efforts.

Progress to date may be summarized as follows:

1. An analytical model of LPG loading systems has been constructed and exercised. The model has been shown to adequately predict the overall performance of LPG loading systems (time-to-load) and the dominant factors to be considered in the design of LPG systems.

2. An LPG laboratory simulator has been designed and built and has been shown to be a useful tool for the evaluation of analytical predictions and for the identification of unpredicted loading system behavior.

3. The analytical model, verified by the experiments, has been used to provide design guidelines for the estimation of LPG loading system performance as a function of various design parameters.

These developments are discussed in detail in subsequent sections of this report. The report is concluded with a summary of results and recommendations for future work in the subject area of investigation.

II. ANALYTICAL MODEL

Analytical efforts have been aimed at developing a model for the behavior of a liquid as it is pumped from an injector, through a system of connecting lines and valves, into the breech. Although continuing analytical work will endeavor to treat this behavior in some detail (including, for example, propagation of pressure waves and local occurrences of cavitation), the complexity of the process has dictated a quasi-lumped parameter approach for initial studies. As shown in the sketch below, the fluid is considered to be made up of three slugs occupying the injector, connecting lines, and breech. The present dynamic analysis takes into account the transfer of fluid from one region to another in response to a step input in pressure at the injector head end.

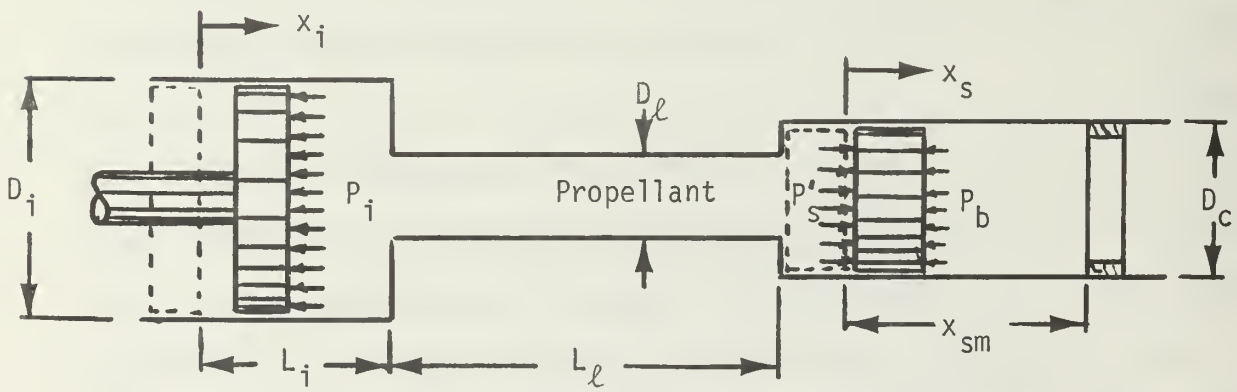

In order to conform with current design concepts, including the design of the laboratory simulator, the system is modeled in the "projectile-ram mode" in which the breech is the same diameter (nominally) as the bore. The model may be easily extended to the "flow-thru" mode of chamber filling by (in the first approximation) simply neglecting the mass of the slug.

A. CONSTITUENT RELATIONSHIPS

1. Injector inertia: The loss in pressure across the moving injector mass (see sketch) may be obtained from the force balance:

$$P_r A_r - P_i A_i = m_p \ddot{x}_i + k_{fp} \dot{x}_i + k_{sp} x_i + F_p \tag{1}$$

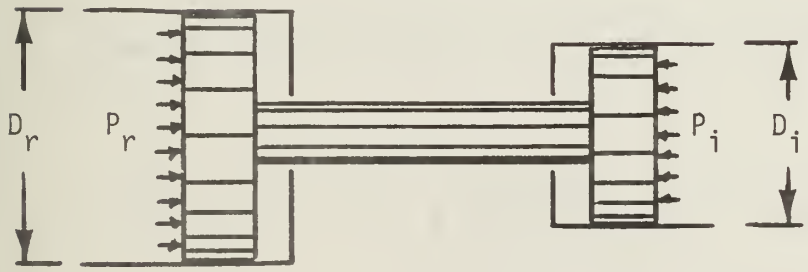

2. Losses in the liquid: In this region there must be a pressure drop to overcome both the inertia and drag of the liquid. Thus, in the injector

$$\Delta P_i = \rho(L_i - x_i)\ddot{x}_i + \rho f_i \frac{(L_i - x_i)}{D_i} \frac{\dot{x}_i^2}{2} \tag{2}$$

in the connecting line

$$\Delta P_\ell = \rho L_\ell \ddot{x}_\ell + \rho f_\ell \frac{L_\ell}{D_\ell} \frac{\dot{x}_\ell^2}{2} \tag{3}$$

and in the chamber

$$\Delta P_c = \rho x_s \ddot{x}_s + \rho f_c \frac{x_s}{D_c} \frac{\dot{x}_s^2}{2}$$

In addition, minor losses can be taken into account by writing

$$\Delta P_{m\ell} = \sum_i \Delta P_i = \frac{\rho \dot{x}_s^2}{2} \sum_i k_{mi} \tag{4}$$

where $k_{mi} = \dfrac{\Delta P_i}{\frac{\rho \dot{x}_s^2}{2}}$.

For example, for the drop due to the sudden contraction from the injector to the connecting line, we have (i = 1)

$$\Delta P_1 = \frac{3}{2} \frac{\rho}{2} \dot{x}_\ell^2 = \frac{3}{2} \frac{\rho}{2} \dot{x}_s^2 \left(\frac{\dot{x}_\ell}{\dot{x}_s} \right)^2$$

and $k_{m1} = \dfrac{3}{2} \left(\dfrac{\dot{x}_\ell}{\dot{x}_s} \right)^2$.

Likewise, for orifices occurring in the connecting line, we would obtain (i = 2), for each such occasion,

$$\Delta P_2 = \left(\frac{A_\ell}{C_d A_o} \right)^2 \frac{\rho}{2} \dot{x}_\ell^2 = \left(\frac{1}{C_d C_c} \right)^2 \left(\frac{\dot{x}_\ell}{\dot{x}_s} \right)^2 \frac{\rho}{2} \dot{x}_s^2$$

and $k_{m2} = \left(\dfrac{1}{C_d C_c} \right)^2 \left(\dfrac{\dot{x}_\ell}{\dot{x}_s} \right)^2$.

Invoking the incompressible assumption the velocities can all be written in terms of $\dot{x}_s$. Thus, since the volume flow from the injector must equal the inflow to the chamber,

$$A_i \dot{x}_i = nA_\ell \dot{x}_\ell = A_c \dot{x}_s \tag{5}$$

whence

$$A_i \ddot{x}_i = nA_\ell \ddot{x}_\ell = A_c \ddot{x}_s \tag{6}$$

and

$$A_i x_i = A_c x_s \tag{7}$$

Combining Eqs. (2) through (7), the total pressure drop across the liquid may be written,

$$P_i - P_s' = \rho\ddot{x}_s \left\{\left[L_i - x_s\left(\frac{D_c}{D_i}\right)^2\right]\left(\frac{D_c}{D_i}\right)^2 + \frac{L_\ell}{n}\left(\frac{D_c}{D_\ell}\right)^2 + x_s\right\} +$$
$$+ \frac{\rho\dot{x}_s^2}{2}\left\{\frac{f_i}{D_i}\left[L_i - x_s\left(\frac{D_c}{D_i}\right)^2\right]\left(\frac{D_c}{D_i}\right)^4 + \frac{f_\ell L_\ell}{n^2 D_\ell}\left(\frac{D_c}{D_\ell}\right)^4 + \frac{f_c x_s}{D_c} + \sum_i k_{mi}\right\} \quad (8)$$

3. Pressure drop from reservoir to slug:

By simple manipulation, we have

$$P_r - P_s' = (P_r A_r - P_i A_i)\frac{1}{A_i} + (P_i - P_s') + P_r\left(1 - \frac{A_r}{A_i}\right)$$

so that after applying Eqs. (5) through (7) to Eq. (1), combining with Eq. (8), and collecting terms, the total drop from reservoir to slug is

$$\frac{P_r - P_s'}{P_r} = 1 - P_s = k_1 + k_2\ddot{x}(H_1 + H_2 x) + k_3\dot{x}^2(H_3 + H_4 x)$$
$$+ k_4\dot{x} + k_5 x + k_6 \quad (9)$$

where $P_s = \frac{P_s'}{P_r}$, $x = \frac{x_s}{x_{sm}}$, and

$$k_1 = 1 - \left(\frac{D_r}{D_i}\right)^2 \qquad k_4 = \frac{k_{fp}\, x_{sm}}{P_r A_c}\left(\frac{D_c}{D_i}\right)^4$$

$$k_2 = \frac{m_s\, x_{sm}}{P_r A_c} \qquad k_5 = \frac{k_{sp}\, x_{sm}}{P_r A_c}\left(\frac{D_c}{D_i}\right)^4$$

$$k_3 = \frac{1}{2}\frac{m_s\, x_{sm}^2}{P_r A_c D_c}\left(\frac{c}{m_s}\right) \qquad k_6 = \frac{F_p}{P_r A_c}\left(\frac{D_c}{D_i}\right)^2$$

$$\frac{c}{m_s} = \frac{\rho x_{sm} A_c}{m_s} \quad \text{(the charge-to-mass ratio)}$$

$$H_1 = \frac{m_p}{m_s}\left(\frac{D_c}{D_i}\right)^4 + \frac{c}{m_s}\left[\frac{L_i}{x_{sm}}\left(\frac{D_c}{D_i}\right)^2 + \frac{L_\ell}{n x_{sm}}\left(\frac{D_c}{D_\ell}\right)^2\right]$$

$$H_2 = \left[1 - \left(\frac{D_c}{D_i}\right)^4\right]\frac{c}{m_s}$$

$$H_3 = f_i \frac{L_i}{x_{sm}}\left(\frac{D_c}{D_i}\right)^5 + \frac{f_\ell}{n^2}\frac{L_\ell}{x_{sm}}\left(\frac{D_c}{D_\ell}\right)^5 + \frac{D_c}{x_{sm}}\sum_i k_{mi}$$

$$H_4 = f_c - f_i\left(\frac{D_c}{D_i}\right)^7$$

4. Drop across the slug:

Again, writing a force balance,

$$P_s' A_c = m_s \ddot{x}_s + k_{fs}\dot{x}_s + k_{ss}x_s + F_s + P_b A_c$$

or $$P_s = k_2 \ddot{x} + k_7 \dot{x} + k_8 x + k_9 \qquad (10)$$

where:

$$k_7 = \frac{k_{fs} x_{sm}}{P_r A_c}, \quad k_8 = \frac{k_{ss} x_{sm}}{P_r A_c}, \quad K_9 = \frac{F_s}{P_r A_c} + \frac{P_b}{P_r}.$$

Equations (9) and (10) are the governing differential equations for the slug position and slug-face pressure as a function of time. In subsequent sections, we have developed solutions for these equations under the initial conditions

$$x(0) = \dot{x}(0) = 0$$

B. SOLUTIONS TO THE GOVERNING EQUATIONS

Equations (9) and (10) have been combined and programmed for solution on the analog computer. This mode of solution has been chosen because of the ease of parameter variation made possible by the analog method. The analog computer solution is outlined in Section IV of this report. In this subsection, several closed form solutions are presented as they are especially useful for the special cases treated.

1. Solution of the semi-linear case. Combining Eqs. (9) and (10), we obtain, upon elimination of P,

$$k_2\ddot{x}(1+H_1+H_2x) + k_3\dot{x}^2(H_3+H_4x) + (k_4+k_7)\dot{x} + (k_5+k_8)x = 1-(k_1+k_6+k_9) \quad (11)$$

This expression is non-linear due to the fluid friction term (preceded by k_3) and the terms accounting for the shift of fluid from the injector to the chamber (terms preceded by H_2 and H_4). An important simplification can be made if the system design parameters are such that

$$\frac{H_4}{H_3} << 1 \ , \quad \frac{H_2}{1 + H_1} << 1$$

and if

$$k_5 + k_8 << 1.$$

The first set of inequalities requires that the difference between the velocity and acceleration of the fluid in the chamber and of that in the injector is small or that piston mass and connecting line effects dominate the system. The second inequality neglects spring effects in the piston and slug behavior. Both of these conditions represent real (but not necessarily desirable) situations and, in fact, are close approximations to the conditions of the experiments

described in Section III of this report. With these simplifications we have,

$$k_2(1 + H_1)\ddot{x} + k_3 H_3 \dot{x}^2 + (k_4+k_7)\dot{x} = 1 - (k_1+k_6+k_9)$$

$$\dot{x}(0) = x(0) = 0$$

This is a Riccati differential equation with the solution

$$x = A \ln \frac{\cosh B(t+t_o)}{\cosh Bt_o} - Ct \tag{13}$$

$$\dot{x} = AB \tanh B(t+t_o) - C$$

$$\ddot{x} = AB^2 \operatorname{sech}^2 B(t+t_o)$$

where $$A = \frac{k_2(1+H_1)}{k_3H_3}, \quad B = \frac{\sqrt{q}}{2k_2(1+H_1)}, \quad C = \frac{k_4+k_7}{2k_3H_3}$$

$$q = (k_4+k_7)^2 + 4\left[1 - (k_1+k_6+k_9)\right](k_3H_3)$$

$$t_o = \frac{1}{B} \tanh^{-1} \frac{(k_4+k_7)}{\sqrt{q}}$$

The variation of pressure P with time may be obtained by substituting Eq. (13) into Eq. (9) or Eq. (10), but this rather laborious procedure has been omitted in deference to the slavishness of the computer.

A most useful application of Eq. (13) is to use it to estimate the time-to-load, t_f. When $t = t_f$, $x_s = x_{sm}$ or $x = 1$, so that

$$1 = A \ln \frac{\cosh B(t_f + t_o)}{\cosh Bt_o} - Ct_f$$

Under the further approximation (also applicable) that piston and slug damping forces are negligible, we have $C \to o$ and $t_o \to o$, giving

$$t_f = \frac{1}{B'} \cosh^{-1} \exp \frac{1}{A} \tag{14}$$

where

$$B' = \frac{\{[1 - (k_1 + k_6 + k_9)] (k_3 H_3)\}^{1/2}}{2k_2(1 + H_1)}$$

Each of the terms in this expression contain design parameters. In particular, it can be immediately seen that

$$t_f \propto \frac{1}{B'} = \left(\frac{2 m_s D_c}{P_r A_c}\right)^{1/2} \frac{1 + H_1}{\left\{\left(\frac{c}{m_s}\right) H_3 \left[\left(\frac{D_r}{D_i}\right)^2 - \frac{P_d}{P_r}\right]\right\}^{1/2}} \tag{15}$$

where H_1 and H_3 are defined with Eq. (9) and P_d is an effective back pressure due to static drag and back pressure given by

$$P_d = \frac{F_p}{A_i} + \frac{F_s}{A_c} + P_b$$

The value of $B't_f$ given by Eq. (14) is plotted in Fig. 1. These expressions will receive additional attention in the discussion of the experiments.

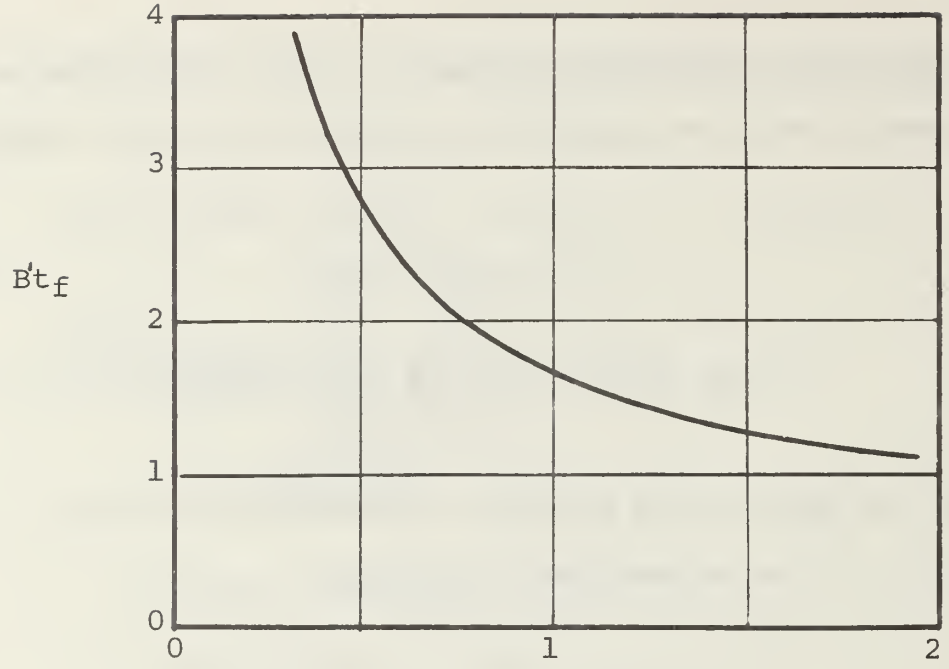

Figure 1.

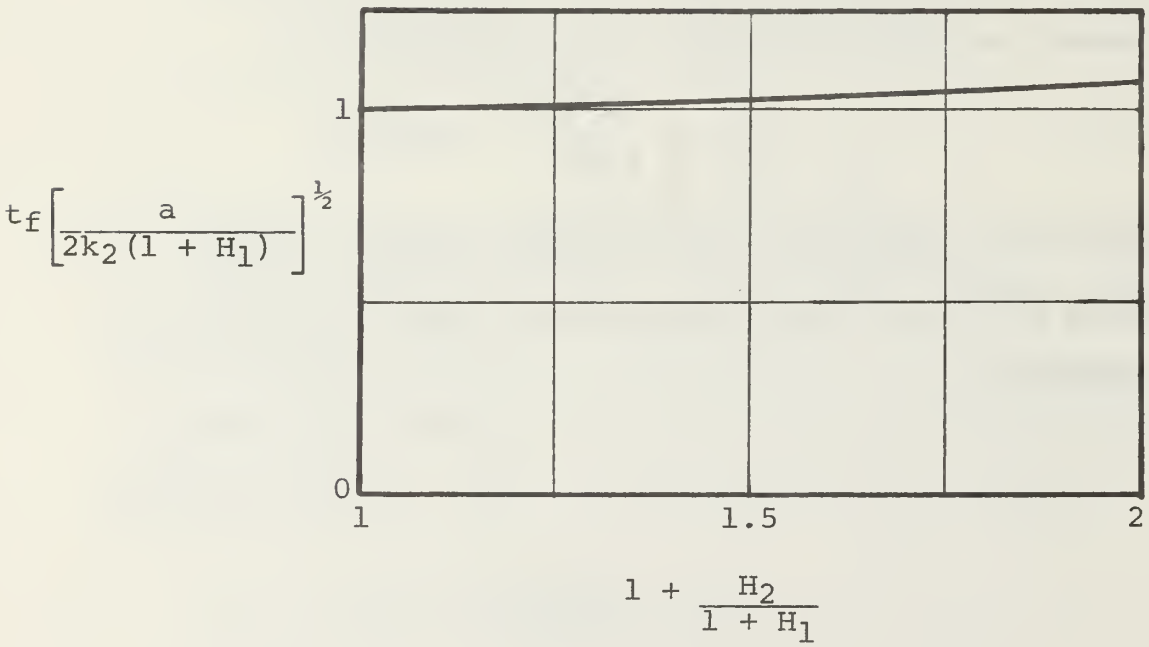

Figure 2.

2. Other closed form solutions: Other less realistic simplifications can be made to Eq. (11) and these are listed here for completeness. Further details are given in Appendix B.

a. Inertia effects only: Here,

$$k_2 \ddot{x} (1 + H_1 + H_2 x) = a$$

$$\text{where } a = 1 - (k_1 + k_6 + k_9) = \left(\frac{D_r}{D_i}\right)^2 - \frac{P_d}{P_r}$$

The solution, developed in Appendix B, is:

$$t = \left(1 + \frac{H_2}{1 + H_1} x\right) \left[\frac{2k_2 (1 + H_1)}{a}\left(\frac{1 + H_1}{H_2}\right)\right]^{1/2} D(u)$$

where D(u) is Dawson's integral [21]

$$D(u) = e^{-u^2} \int_0^u e^{t^2} dt$$

$$\text{and, } u = \left[\ell n \left(1 + \frac{H_2}{1 + H_1} x\right)\right]^{1/2}$$

Setting x = 1 we have, for the ram time

$$t_f \left[\frac{a}{2k_2(1 + H_1)}\right]^{1/2} = \left(1 + \frac{H_2}{1 + H_1}\right)\left(\frac{1 + H_1}{H_2}\right)^{1/2} D(u) \qquad (16)$$

This result is plotted in Fig. 2 for representative values of $1 + \frac{H_2}{1 + H_1}$.

Note that H_2 is a measure of the nonlinearity contributed by the difference in acceleration of the liquid between injector and piston ($H_2 = 0$ if $D_c = D_i$). Figure 2 shows the very small effect of this factor for the acceleration only case. Therefore, if this case is a reasonable approximation to Eq. (11), it is also reasonable to write

$$K_2 \ddot{x}(1 + H_1) = a, \text{ so that}$$

$$t = \left[\frac{2k_2(1 + H_1)}{a} x\right]^{1/2}$$

$$\text{and} \quad t_f \left[\frac{a}{2k_2(1 + H_1)}\right]^{1/2} = 1 \qquad (17)$$

as seen in Fig. 2.

b. Fluid friction only: In this case, Eq. (11) becomes

$$k_3 \dot{x}^2 (H_3 + H_4 x) = a$$

and

$$t = \frac{2}{3}\left(\frac{H_3}{H_4}\right)\left(\frac{k_3 H_3}{a}\right)^{1/2}\left[\left(1 + \frac{H_4}{H_3} x\right)^{3/2} - 1\right] \qquad \text{(Appendix B)}$$

so that

$$t_f \left(\frac{a}{k_3 H_3}\right)^{1/2} = \frac{2}{3} \frac{H_3}{H_4}\left[\left(1 + \frac{H_4}{H_3}\right)^{3/2} - 1\right] \qquad (18)$$

Since H_4 is essentially equal to f_c, the friction coefficient for the chamber, it is not likely to have a value larger than about 0.05. H_3 is of the order of magnitude of 1 (in the experimental apparatus it is about 3.3) so that it is unlikely that H_4/H_3 would be larger than 0.05 in which case $t_f (a/k_3 H_3)^{1/2} = 1.0124$. Thus, it is seen

again that the nonlinearity contributed by the const.(x) term, as in the acceleration case, is relatively insignificant. With this approximation, we may write

$$k_3 H_3 \dot{x}^2 = a, \text{ so that}$$

$$t = x\sqrt{\frac{k_3 H_3}{a}}$$

$$\text{and } t_f = \sqrt{\frac{k_3 H_3}{a}} \tag{19}$$

This result is all the more useful in comparing the linearized versions of the acceleration only and fluid friction only cases. Thus,

$$R = \frac{\text{ram time, acceleration only}}{\text{ram time, fluid friction only}} \Bigg| \text{ linearized} = \left[\frac{2k_2(1 + H_1)}{k_3 H_3}\right]^{1/2} \tag{20}$$

which is a valuable ratio in analyzing the extent to which a system design is limited by inertia or by fluid friction effects.

c. Completely linearized system: If the fluid friction is completely neglected, along with H_2, the result is the familiar linear damped spring-mass expression:

$$k_2 \ddot{x} (1 + H_1) + (k_4 + k_7) \dot{x} + (k_5 + k_8) x = a$$

with the solution

$$x = \frac{a}{k_5 + k_8} \left\{ 1 + \frac{e^{-\zeta\omega_n t}}{\sqrt{1 - \zeta^2}} \sin \left[\omega_n \sqrt{1 - \zeta^2}\, t + \alpha\right] \right\} \tag{21}$$

$$\alpha = \tan^{-1} \frac{-\sqrt{1 - \zeta^2}}{-\zeta}$$

where $\omega_n^2 = \dfrac{k_5 + k_8}{k_2 (1 + H_1)}$ and $2\zeta\omega_n = \dfrac{k_4 + k_7}{k_2(1+H_1)}$

Since no accurate values for k_5, k_8, k_4, and k_7 were available at the time of this writing (in the experimental apparatus, these values are essentially zero), this solution has not been analyzed in any great detail. In fact, our results indicate that these damping and spring terms do not significantly affect the performance of an LPG loading system when compared with the similar effects present in the compressible (gas) side of the system.

In the following section of this report these closed-form solutions are compared with the experimental results. As has been mentioned, the complete solution to the governing differential equations has been obtained by analog computer methods and is discussed in Section IV of this report.

III. EXPERIMENTAL PROGRAM

A. DESIGN OF THE EXPERIMENTAL APPARATUS

After a review of the available background literature and current research efforts, work was begun to design and fabricate a laboratory model capable of simulating the dynamic behavior of a liquid propellant feed system for a 20mm gun firing at a rate of up to 1,000 rounds per minute. The selection of a 20mm bore diameter was dictated by considerations of laboratory capabilities and was not due to a desire to accurately simulate an operational system. The concept criteria coupled with the unique requirements for an accurate laboratory simulation resulted in the establishment of the following initial design parameters:

chamber volume (variable)	50-70cc
maximum operating frequency	17hz
water flow rate (maximum)	75.5gpm
maximum chamber pressure	1500psi
desired maximum time to fill chamber	15ms

Due to the time constraints involved, it was felt that off-the-shelf items should be used whenever possible. The 20mm bore-diameter chamber was loaded with a brass slug weighing 93 grams which rode on two graphite filled Teflon sealing rings. The brass slug, which simulated the projectile, was cycled from the breech end of the chamber to the barrel end and returned to the breech end, completing one hypothetical firing cycle. To facilitate visual inspection of the bore and slug, the test chamber itself was fabricated from a three-inch O.D. Lucite cylinder, 18 inches long, bored to a 20mm inside diameter and fitted with aluminum end caps. The entire chamber assembly is held together with four tie rods and cap screws, as shown in Figs. 3 and 4.

Figure 3. Experimental Apparatus

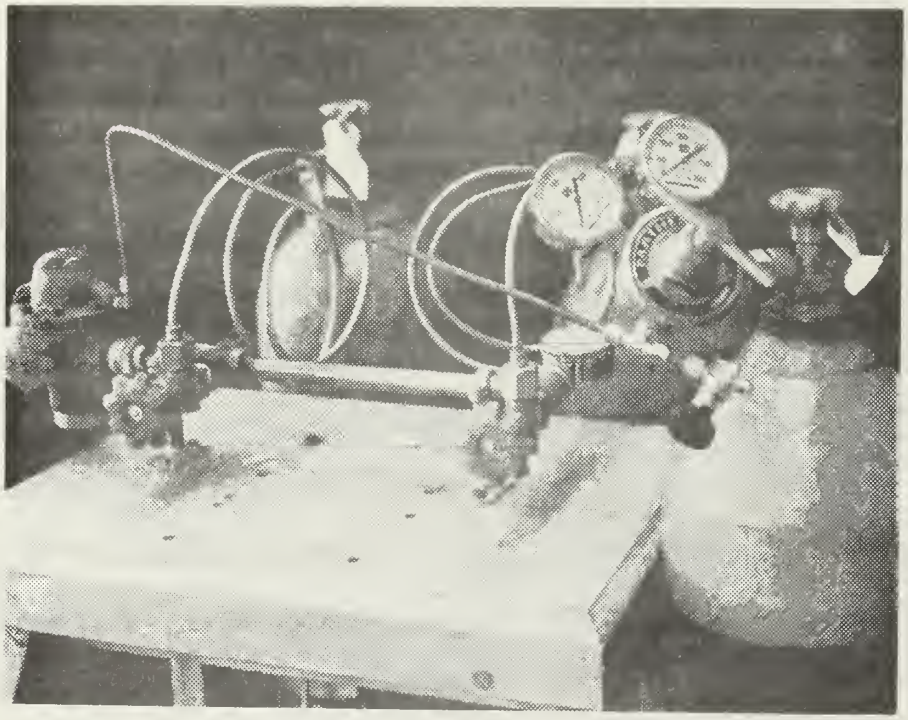

Figure 4. Gas Supply System

Because of the desire to vary the charge to mass ratio, a variable chamber volume was necessary. To accomplish this with one chamber, a volume control retaining rod was designed into the system. This brass rod, bored to allow gas to pass its length, was threaded through a plate which was attached to the barrel end cap holding the rod in the chamber. The rod, which has a Teflon disc on the end, not only established the volume of the test chamber, but provided a buffer stop for the slug at the end of its forward motion. Another Teflon buffer was affixed to the breech end cap to cushion the slug in return motion.

The initial design concept started a simulated firing cycle with a slug at the breech end of the empty chamber, as shown in Fig. 5. This is the ready-to-ram position. The simulated propellant was then introduced, ramming the slug to the opposite (barrel) end of the chamber as the chamber is filled. This was accomplished by applying gas pressure to a power piston which drove an injection piston. The injector piston forced the propellant past a flow check valve and into the chamber. This placed the slug in the ready-to-fire or in-battery position. In an actual gun, the propellant would be ignited at this time in the cycle. Due to the laboratory constraints, the water expulsion system was used.

With the slug at the in-battery position, ram gas pressure on the power piston was vented and return gas pressure applied to both the power piston and the muzzle end of the test chamber (Fig. 6). At the same time, gas pressure was applied to a pilot-operated check valve, the dump valve, to open it. With the dump valve open and reverse flow in the feed line eliminated by the flow check valve, the gas pressure on the muzzle end of the chamber forced the slug to the breech end,

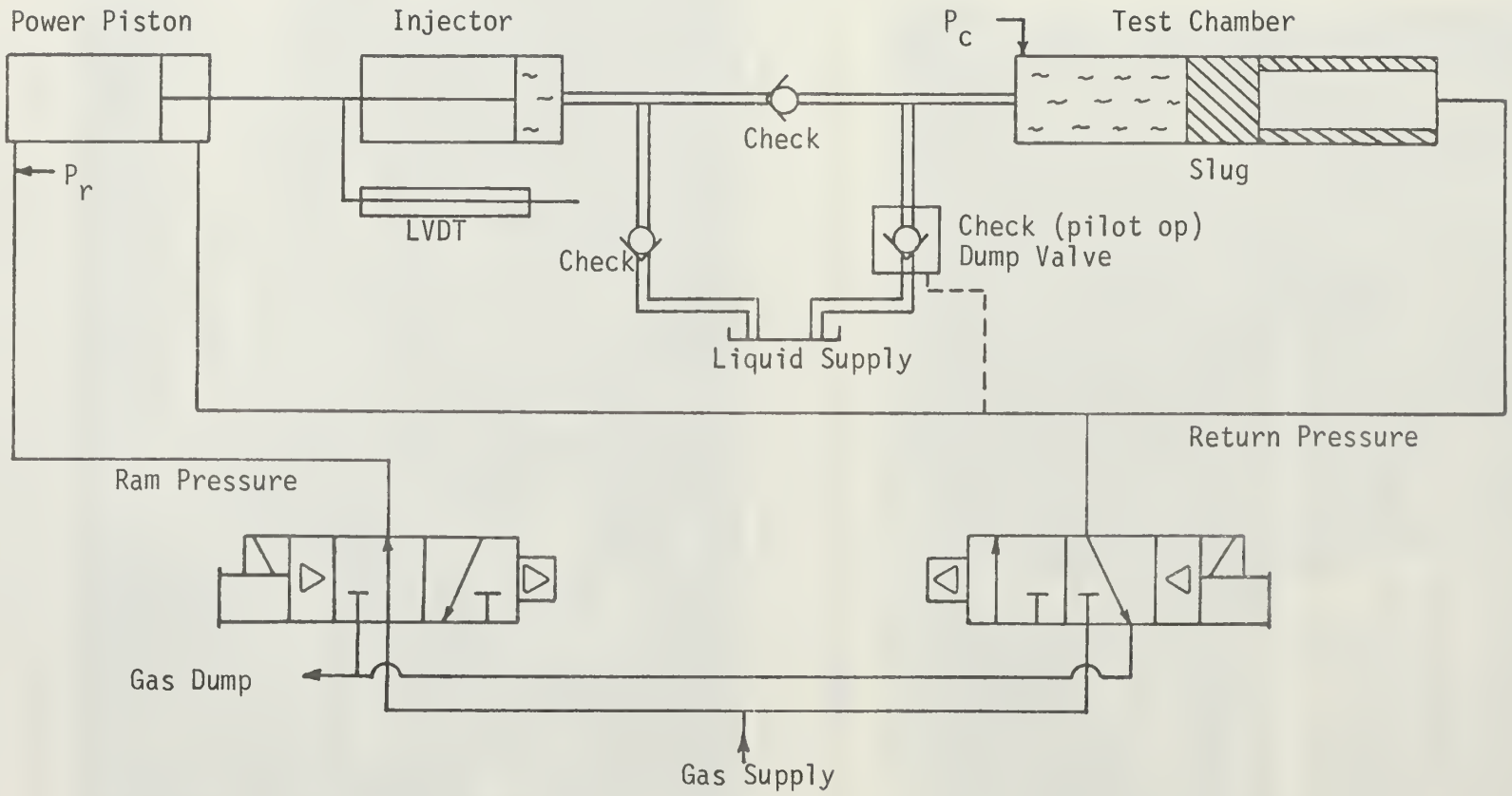

Figure 5. Pneumatic control system in ram position.

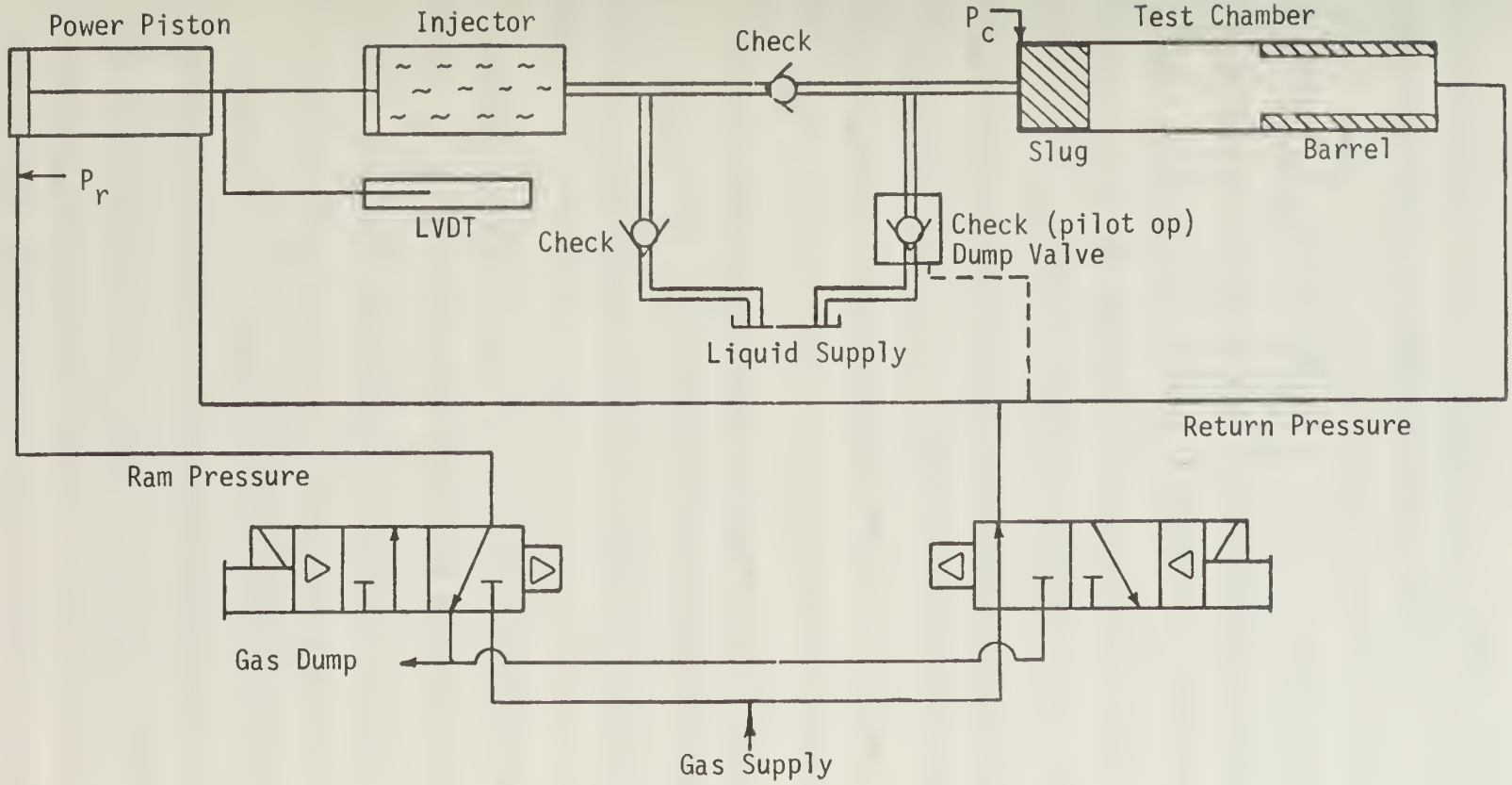

Figure 6. Pneumatic control system in return position.

expelling the propellant through the dump valve. At the same time, with the power piston and injector piston moving to the rear, another shot of fluid was drawn into the injector from the supply line. To repeat the ram stroke, the gas pressure was vented to atmosphere.

Since the timing and synchronization of the gas and liquid flows were critical to the success of the experiment, a single control mechanism was desired. With this in mind, an integrated gas and liquid system was designed. It was initially thought that balanced spool valves could be used to control one or both ends of the system. However, obtaining off-the-shelf stock for such specialized requirements (the necessary low response times and high flow rates) presented scheduling difficulties which were unacceptable. It was discovered that normally open and normally closed solenoid operated gas spool valves were "readily" available for operating pressures up to and including 150psi and could be obtained with modifications allowing operation up to 250psi.

A system was designed using one valve to control the ram gas pressure and one valve to control the return gas pressure. By using two valves, one normally open and one normally closed, gas pressure could be applied to either the ram or the return line with the other line being vented by energizing or de-energizing the appropriate solenoids by means of a single relay. By connecting the pilot line of the dump valve to the return gas line, the entire feed system could be controlled with one electrical switch, or each valve could be energized and de-energized separately. This control system would also allow maximum flexibility for future efforts with little modification. Through an easily constructed

electrical timing circuit, automatic ram and return cycling could be accomplished for simulation of burst firing.

B. CONDUCT OF THE EXPERIMENT

The assembled experimental LPG simulator is shown in Fig. 7. A linearly variable differential transformer (LVDT) was manufactured and mounted next to the injector piston. This LVDT was attached to the connecting rod, between the power piston and the injector piston. The volume of the liquid being placed under pressure during each shot was measured by filling the system in the ready-to-ram position and then draining it into a graduated beaker. By measuring the displacement of the injector piston head with the LVDT, the volumetric rate of fluid injection during the ram stroke was obtained.

Five pressure taps were drilled in the test chamber. Two of these taps were located as close to the breech end as possible, one at 20 degrees from top center and the other at 20 degrees from bottom center in a counterclockwise direction, as seen from the breech end of the chamber. The remaining three taps were placed two inches, three and one-half inches, and five inches from the breech end, in line with the first bottom tap.

It was discovered during operation that when the slug was returned to the ready-to-ram position, it would wipe some of the liquid out of these last three taps. In the next ram cycle, bubbles of gas which had replaced the liquid would distort the pressure response of these taps. To expedite the investigation, these three taps were plugged and only the taps closest to the breech were used.

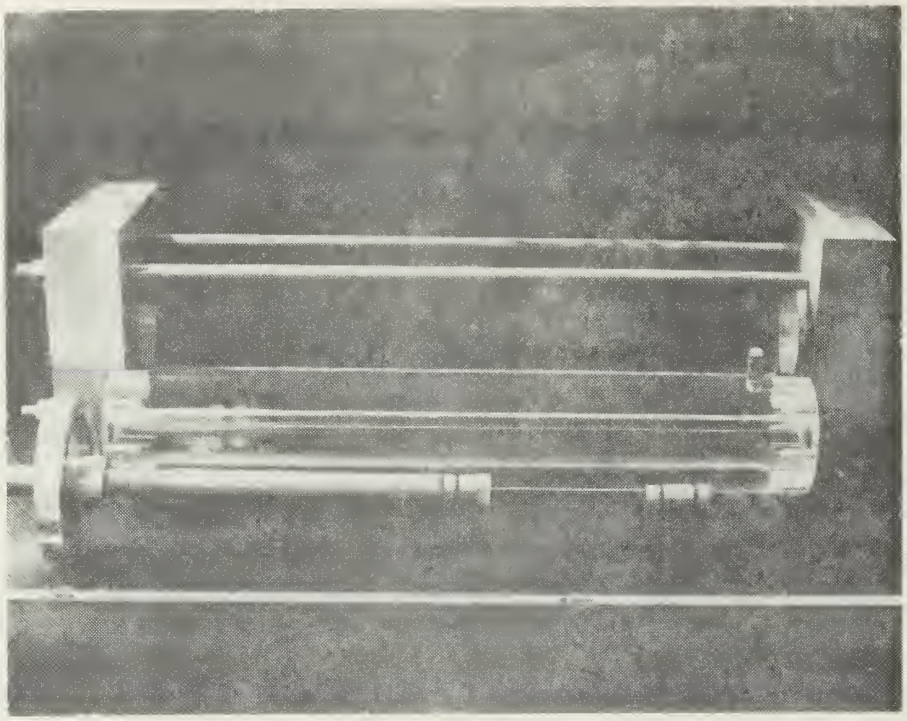

Figure 7. Chamber Disassembled

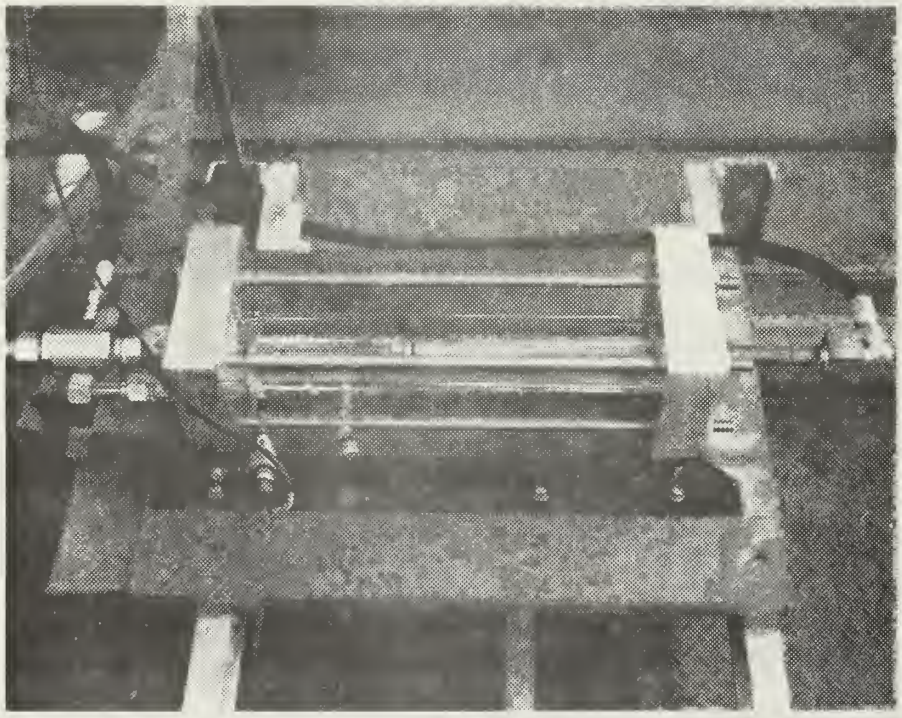

Figure 8. Chamber Assembled

A 4-channel Hewlett-Packard 3960 Magnetic Tape Recorder was used to FM record desired data during system operation. Kaman diaphragm type (1000psi) pressure transducers were connected to the two breech pressure taps on the test chamber. The pressure signals were processed with a Kaman Digi-Vit Readout Unit which also provided a visual (digital) display. Since the maximum output of the Digi-Vit unit was one volt, the breech pressure signals were amplified through Sanborn 8875A Differential Amplifiers prior to being recorded. The LVDT excitation signal was obtained by using a Hewlett-Packard Model 200CD Oscillator. The output of the LVDT was passed through a voltage divider circuit and then recorded on the tape.

A Brush Recorder (Mark 280) was used to obtain a visual display of the recorded data. By transcribing the desired signals on the Magnetic Tape Recorder at a tape speed of 15 feet per minute and playing them back into the Brush Recorder at 3-3/4 feet per minute, the time scale of the output was expanded by a factor of four on the Brush recordings (viz., from a real-time maximum of 200mm/sec to a delayed time maximum of 800mm/sec.). Two pressures and the LVDT reading were recorded for each shot.

Before each shot at a new ram gas pressure, calibration points were marked on the Brush chart to establish the full-scale deflection pressures for each transducer during the shot. The LVDT full-scale deflection was maintained at 40 divisions by adjusting the amplitude and frequency of the oscillator. A slug stroke of five inches was held constant throughout the experiment.

To eliminate the possibility of particulate contamination of the water, a 25 gallon tank of distilled water was connected to the discharge of the dump valve. This return line was elevated to place a hydrostatic head of approximately one psi on the discharge side of the dump valve to prevent gravity draining and to eliminate air ingestion in the chamber and connecting line when the dump valve was open.

Data were obtained for nominal supply pressures ranging from 50psig to the system limit of 220psig as indicated at the gas supply system regulator (Fig. 8). Further detailed descriptions of the experimental apparatus and procedures are documented in a previous report [22].

C. EXPERIMENTAL RESULTS

1. Chamber pressure: Ram displacement, chamber pressure, and ram gas pressure (driving pressure) were recorded for driving pressures between 50psig and 220psig in 10psi increments. Typical results are presented in Figs. 9-12. In these figures, the recorder outputs have been arranged so that a vertical line crosses each trace at a corresponding time during the event. Event time increases from left to right with one centimeter equating to 12.5 milliseconds. Ram time has been defined as the time interval which starts when the ram gas pressure trace deviated from the horizontal to the point in time when any discernable volumetric increase ceases, as shown in Fig. 9.

After application of driving pressure to the power piston, a time lag was evident before the piston was set in motion. This time lag was largely due to static friction forces acting on the pistons and the slug.

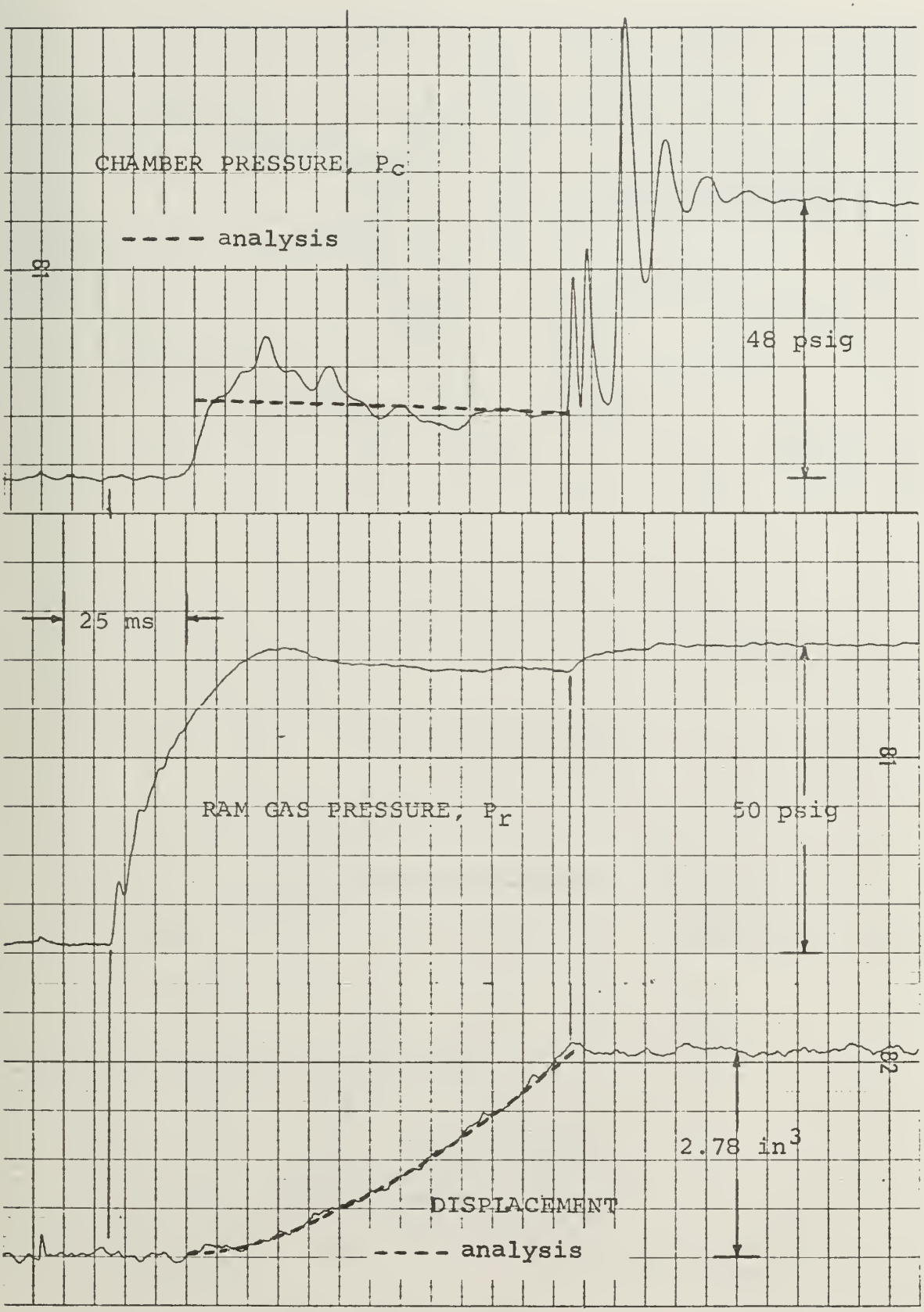

Figure 9. Typical responses, P_r=50.

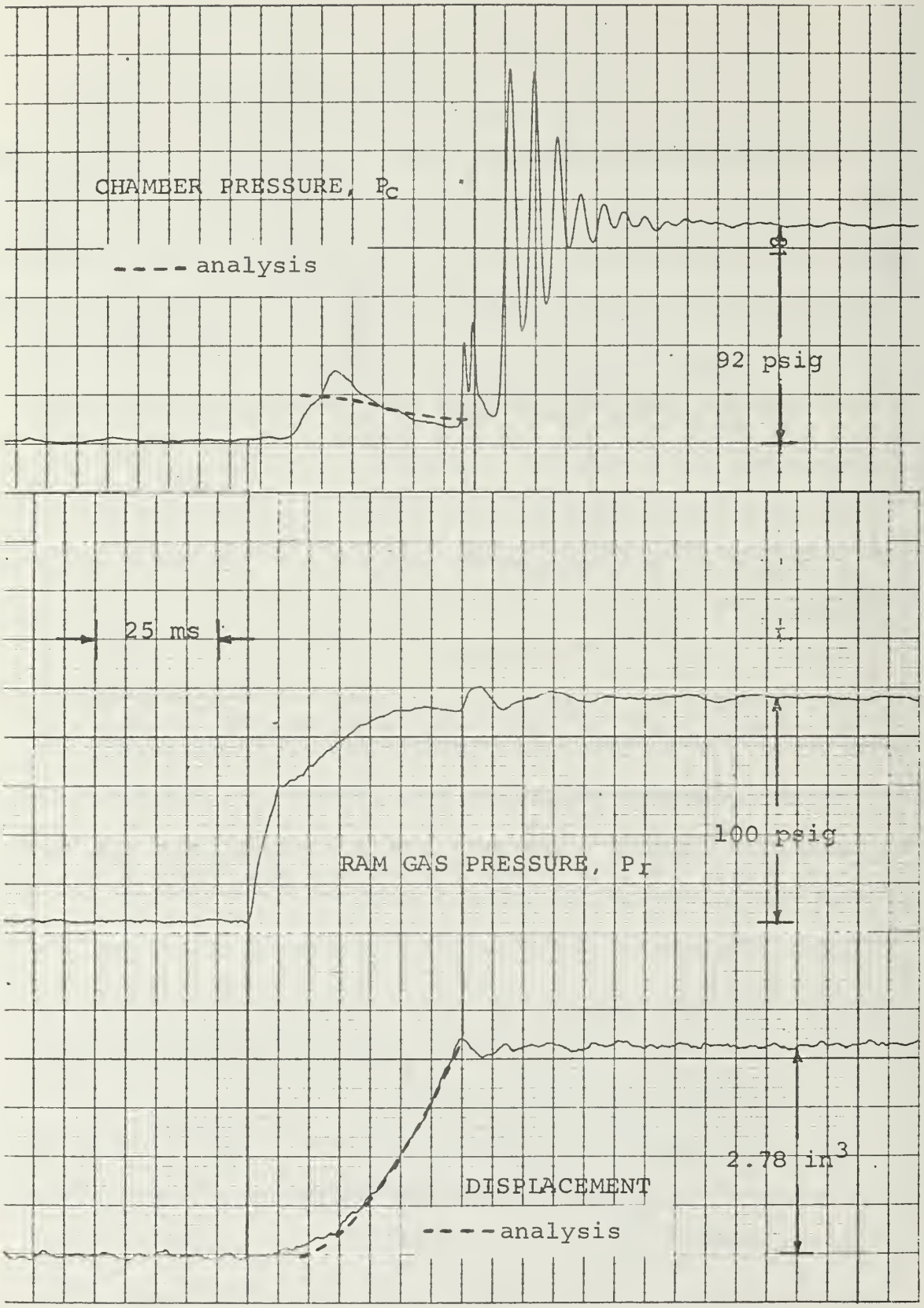

Figure 10. Typical responses, P_r= 100.

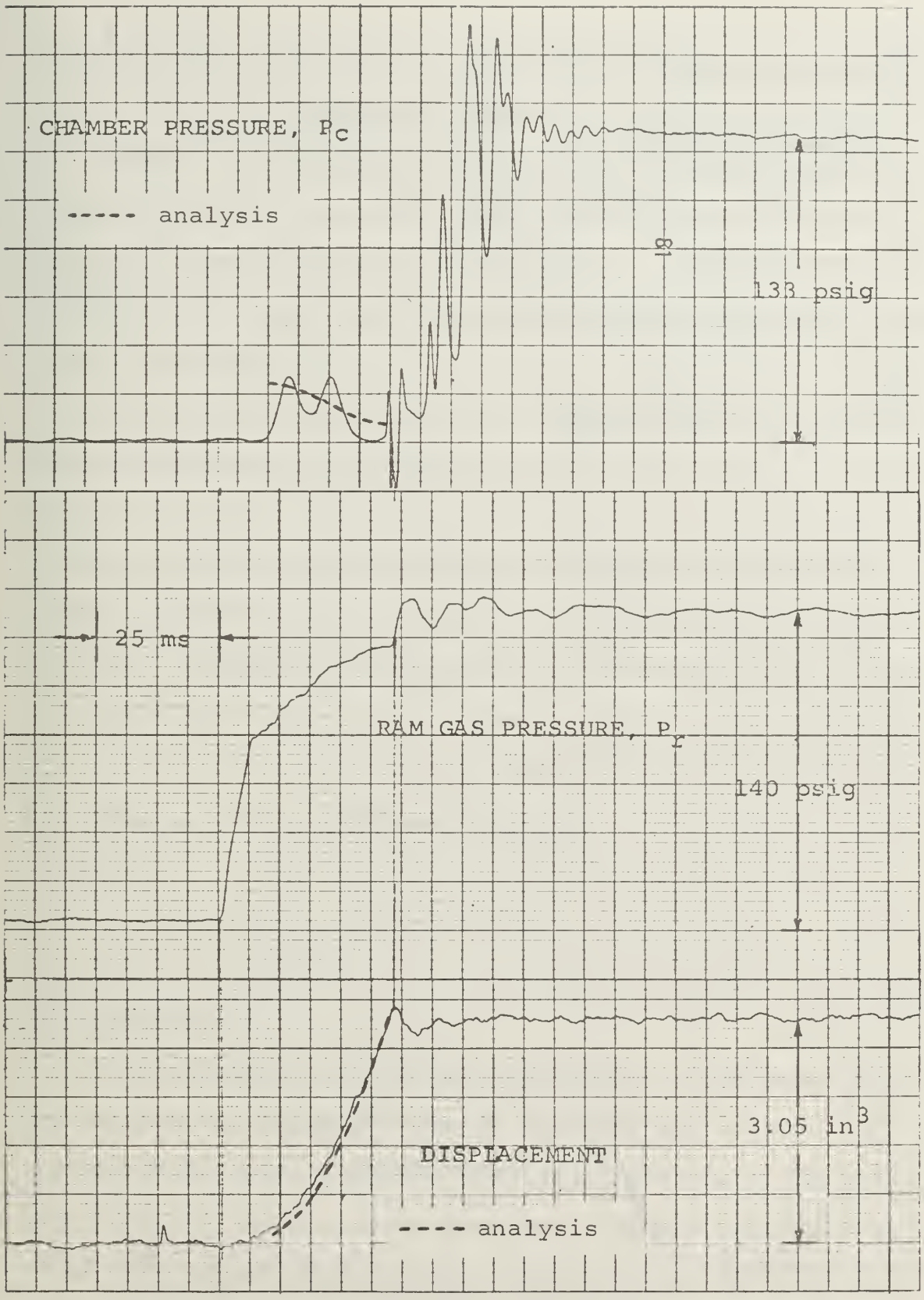

Figure 11. Typical responses, P_r= 140.

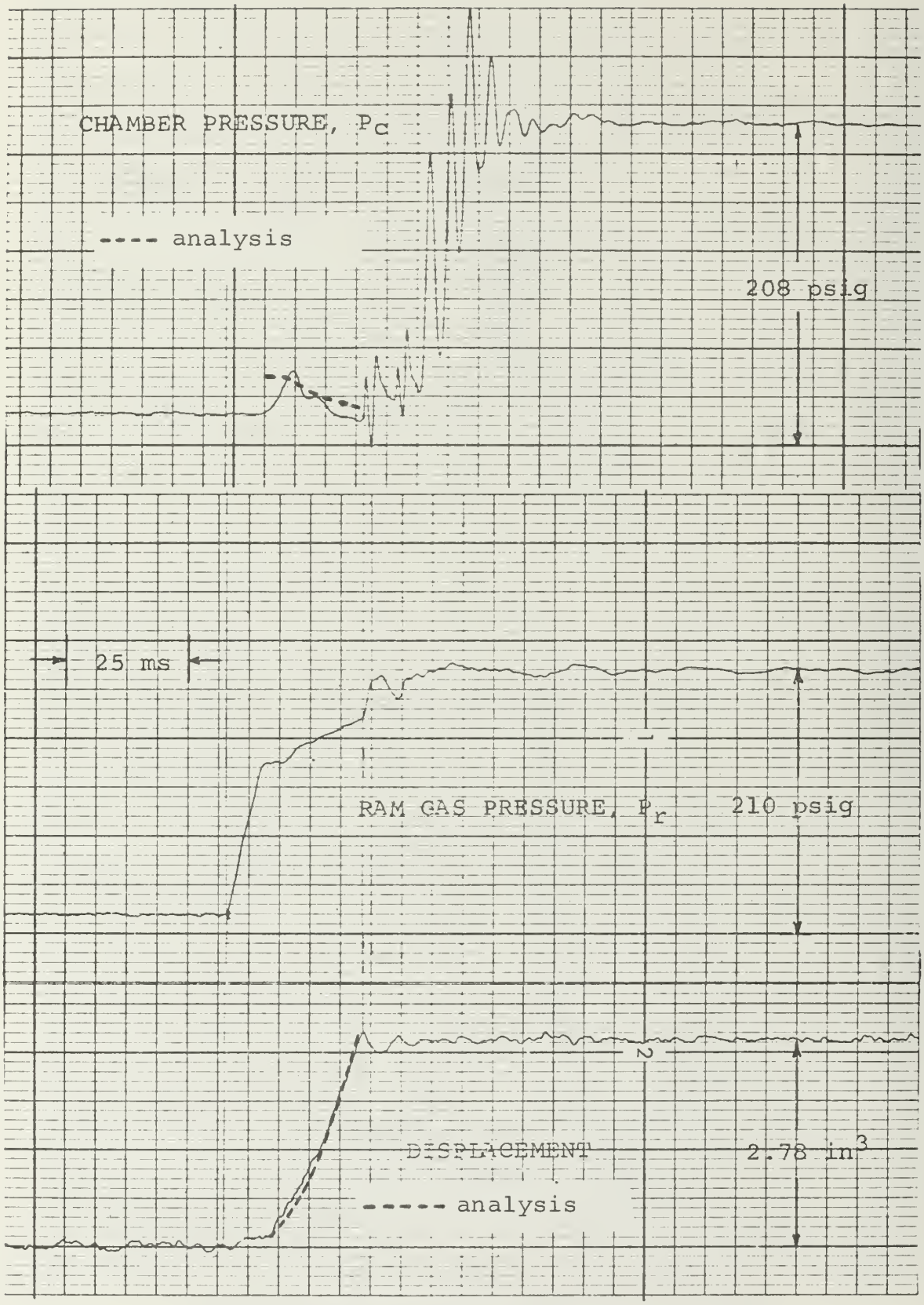

Figure 12. Typical responses, P_r= 210.

After an initial rapid increase of the driving pressure, these frictional forces were overcome, and injection of the fluid and, hence, the ramming of the slug proceeded. The relatively gradual increase in driving pressure after piston motion started has been attributed to losses in the upstream valving and connecting lines and the resultant inability of the supply system to provide an adequate flow of gas to the power piston chamber.

During the ram stroke, the chamber pressure exhibited some characteristics which were not completely predictable by the analytical model in its present form. After an initial increase, the chamber pressure tended to decrease as the slug preceded the fluid column down the chamber. To facilitate the discussion of these pressure fluctuations, one must first observe the behavior of the displacement trace. In addition to being a measure of the volume of fluid injected, it is an indicator of fluid velocity and acceleration behavior. As motion starts, the near-zero slope of the trace implies a low velocity which increases as expected. The rapid initial rate at which the slope increases implies a rapid increase in the acceleration. As the ram stroke proceeds, this rate of increase of the acceleration diminishes and the curve becomes more linear.

As demonstrated by the analysis, the pressure difference across the system is mainly influenced by inertia forces and viscous forces. The inertial forces induce a pressure reduction proportional to the acceleration. Likewise, the viscous forces endure a pressure reduction proportional to the square of the velocity. Following the initiation of motion, as the level of acceleration of the fluid and the slug mass

decreases due to friction, the difference in pressure between driving pressure and chamber pressure necessary to provide the acceleration level decreases with an attendant increase in the chamber pressure. Initially, fluid velocities are small so that the pressure difference is due mainly to this large but decreasing acceleration. As the acceleration decreases, the chamber pressure increases until the velocities in the system become significant from a viscous friction point of view. As velocity increases, the loss in pressure due to these viscous effects overcomes the increasing pressure due to the decreasing level of acceleration of the moving solid and fluid masses. The net effect at this point is a loss in chamber pressure.

In several runs (Figs. 9 and 10, for example), the acceleration of the masses dies out after a few milliseconds. In these cases, the expected continuous drop in chamber pressure, due to viscous effects, is observed after the initial pressure peak. In several other runs (Fig. 11, for example), the acceleration effects are present throughout the run. In these cases (typical of higher driving pressures), the velocity of the moving masses increases through a large part of the event. Acceleration levels decrease initially, as before, with the resulting initial rise in chamber pressure. Viscous losses are then evident with the corresponding decrease in chamber pressure.

In a viscous fluid, pressure decreases are proportional to the square of the velocity while the sliding friction losses of the solid mass are more accurately modeled as being proportional to lesser power of the velocity. For a given change in pressure drop across the system, therefore, there is a tendency for the slug to accelerate and decelerate more

rapidly than the fluid. In the present experiment, the slug apparently accelerates at decreasing levels throughout the ramming process; no deceleration of the slug was noted. Thus, the second and subsequent pressure decreases in the chamber, when they occur, are thought to be due to the inability of the fluid column to keep page with the slug. This motion appears to be oscillatory in the P_c curves of Figs. 9-12.

All of the effects discussed here are influencing the motion of the slug and fluid and these remarks are not meant to create an overly simple interpretation of the complex interactions involved. It is also important to note that the chamber pressure is measured at a fixed point at the breech end and that the amount of fluid upstream of this point decreases with time. Thus, the length of the fluid column, upon which inertial and viscous forces are acting, decreases with respect to the location of pressure measurement. This change in length of the column is on the order of 30% in these experiments and tends to decrease pressure drops due to inertial and frictional effects as measured at the fixed pressure taps. The above discussion also assumes that the driving pressure is relatively constant for that portion of the event in which the forces mentioned are acting. The ram gas pressure did indeed behave approximately in this manner at lower pressures. As ram pressure was increased, however, the response deviated more and more from the assumed step input.

2. Terminal behavior and ullage effects: The oscillatory behavior of the chamber pressure after the slug came to rest was due to the expansion and contraction of the entrained gases in the fluid column (Figs. 9-12, for example). At the moderate driving pressures initially

used, the traces resembled second order damped responses and this resemblance prompted a further investigation of this portion of the ram cycle event.

Viewing the dynamic portion of the system as picture in the sketch below, a force balance on the ram and injector pistons at the instant the slug reached the end of its stroke gives $A_p(P_r-P_c) = m_p \ddot{x}_i + k_{fp}\dot{x}_i + k_{sp}x_i$ (see Eq. (1)).

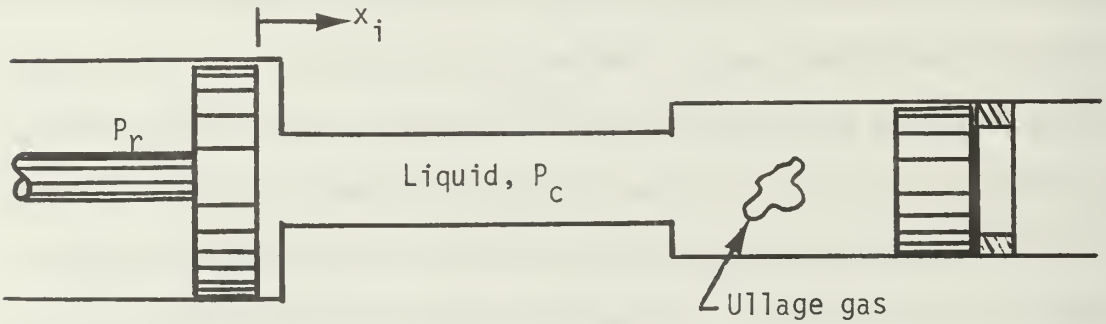

From the definition of the effective bulk modulus, β_e , for a mixture of liquid and ullage gas, the flow due to compliance in the mixture may be written

$$A_p\dot{x}_i = \frac{\forall_t}{\beta_e}\dot{P}_c$$

Neglecting the mechanical spring forces, $k_{sp}x_i$, and combining these expressions to eliminate x_i,

$$P_c = P_r - \frac{\forall_t}{A_p{}^2\beta_e}(m_p\ddot{P}_c + k_{fp}\dot{P}_c)$$

and, after Laplace transformation, and solution with $\dot{P}_c(o) = 0$ and $P_c(o) = P_o$, the pressure variation is found to be

$$\frac{P_c(t) - P_o}{P_r - P_o} = 1 + \frac{e^{-\omega_n \zeta t}}{\sqrt{1 - \zeta^2}} \sin\left(\omega_n \sqrt{1 - \zeta^2}\, t + \phi\right) \qquad (22)$$

where $\phi = \tan^{-1} - \frac{\sqrt{1 - \zeta^2}}{-\zeta}$

$$\omega_n = \left(\frac{A_p{}^2 \beta_e}{m_p \forall_t}\right)^{1/2}$$

$$\zeta = \frac{k_{fp}}{2A_p} \sqrt{\frac{\forall_t}{m_p \beta_e}}$$

and $\forall_t$ = total fluid volume (liquid and ullage)

Equation (22) for a damped linear system is analogous in form to the measured pressure variations following the ramming cycle. The natural frequency and damping coefficient can therefore be obtained from each driving pressure curve by measuring the appropriate amplitudes and the period of oscillation (see Appendix C). Using these experimental values of ω_n and ζ, values for equivalent bulk modulus and friction factor were obtained. The variation in these calculated values were within the limits of uncertainty predicted for most cases [22]. The percentage of entrapped (ullage) gas in the fluid volume is then obtained by using this calculated value of β_e. Trapped gases were found to be on the order of 0.1 to 0.6% of the liquid volume during these tests. As the ram gas pressure was increased for successive runs, the oscillation of the chamber pressure became more erratic as can be seen by comparing Figs. 9 and 10 with Figs. 11 and 12. The validity of the results obtained for ω_n, ζ, β_e, and k_{fp}

at these higher pressures is therefore suspect, even though the general form of the curve repeats at all driving pressures.

In some of the events, the chamber pressure curve indicates a pressure below atmospheric immediately after the slug reaches the end of its travel. These initial low-pressure oscillations are tentatively attributed to slug/fluid interactions as the slug comes to rest against the buffer. Note that following the stopping of the slug, the initial pressure change is always a steep increase, indicating that the fluid column is initially compressed against the stationary slug.

It was hoped that a value of equivalent bulk modulus could be obtained from the displacement trace to correlate the value obtained using Eq. (22). However, electrical noise in the LVDT circuitry produced a signal with such little definition that the extremely small volume changes associated with trapped gas effects were not distinguishable.

3. Ram time measurements: The data displays of ram-time versus ram gas pressure (Fig. 13) portray some rather interesting characteristics. The general trend and validity of the curve is confirmed by the fact that the data presented were taken on several occasions and repeatedly at selected conditions. It should also be noted that for driving pressures above the moderate range ($p_r \approx$ 150psig) the decreases in ram-time are small for increases in ram gas pressure. The scatter of the data can be attributed to the inherent uncertainty encountered in any experimental data taking system, coupled with possible erratic behavior of the pneumatic equipment. Any uncontrolled

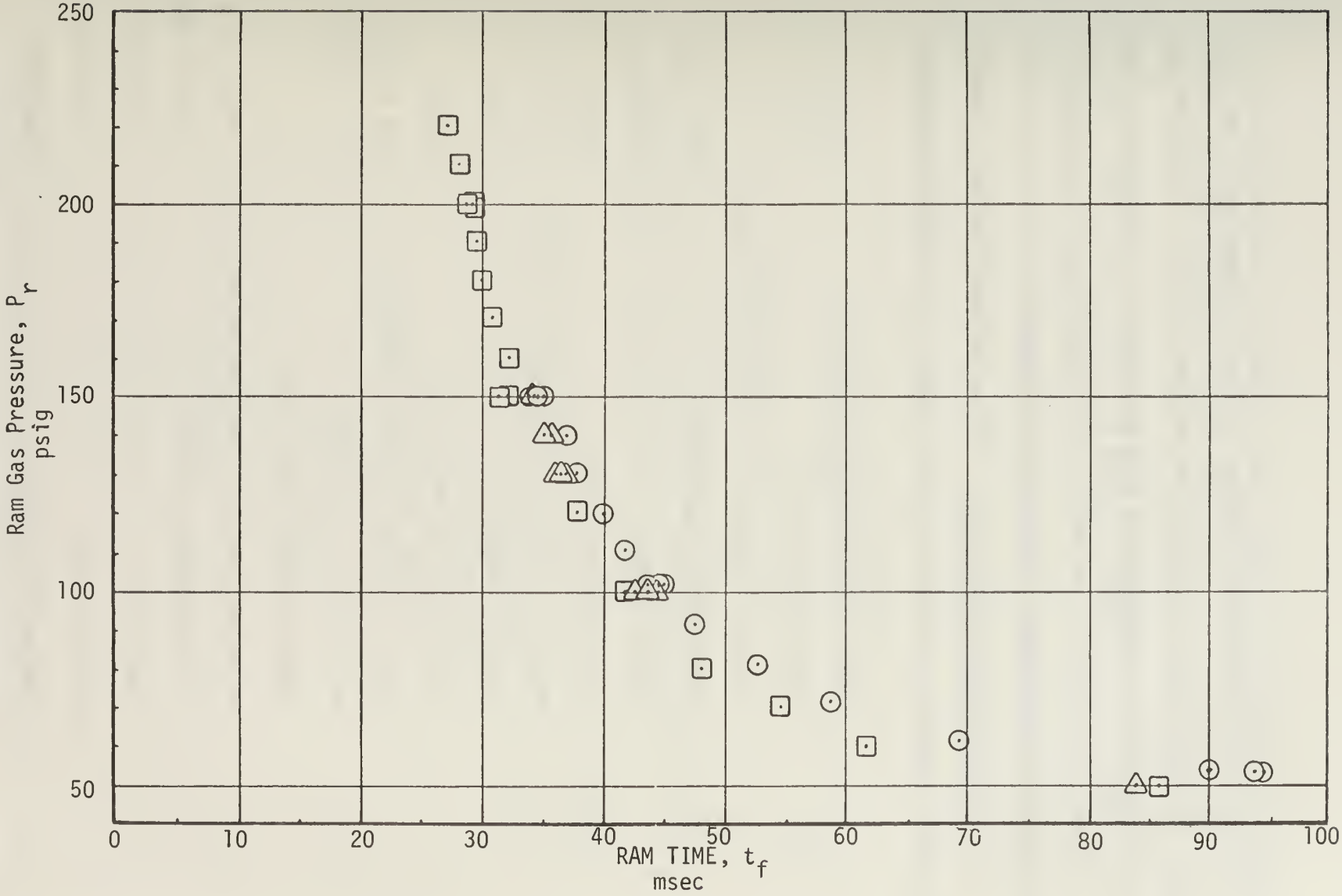

Figure 13. Ram Time vs. Ram Gas Pressure - Experimental

variations in equivalent bulk modulus for the different tests did not appear to significantly influence the ram-time results. An effort was made throughout the experiment to keep the amount of entrapped gas small and relatively constant. The data points conforming to a consistent trend would indicate that this was accomplished.

4. Comparison with predictions: The experiments discussed herein have been conducted with the following values of the design parameters:

A_c	chamber cross-sectional area, in^2	(0.49)
c/m_s	charge-to-mass ratio	(0.43)
D_i	injector diameter, in. (=D_r, in this case)	(1.50)
D_ℓ	connecting line diameter, in.	(0.57)
D_c	chamber diameter, in.	(0.79)
f_i, f_ℓ, f_c	flow friction factors	(0.03)
$k_{fp}=k_{fs}$	mechanical damping coefficient, lb sec/in.	(.001)
L_i	injector length, in.	(1.60)
L_ℓ	connecting line length, in.	(16.0)
m_p	mass of injector piston, lb sec^2/in.	(5.2×10^{-3})
m_s	mass of slug, lb sec^2/in.	(5.3×10^{-4})
n	number of connecting lines	(1)
P_d	equivalent pressure drop due to drag, lb/in^2	(empirical)
P_r	ram gas pressure, $lb/in.^2$	(controlled)
t	time, sec.	(variable)
t_f	ram-time, sec.	(variable)
x_s	slug position, in.	(variable)
x_{sm}	maximum (final) slug position, in.	(5.00)

The sudden decrease in diameter from injector to connecting line gives a minor loss coefficient (see Eq. (4)) of

$$k_{m_1} = \frac{3}{2}\left(\frac{D_c}{D_\ell}\right)^4 = 5.5$$

The entrance to the chamber is constricted by an orifice-type reduction with contraction ratio (C_c) of 0.92. The coefficient for this is (with C_d=0.61)

$$k_{m\,2} = \left(\frac{1}{C_d C_c}\right)^2 \left(\frac{D_c}{D_\ell}\right)^4 = 11.7$$

and $$\sum_i k_{mi} = 17.2$$

These design factors lead to the following values of the relevant parameters for Eqs. (9) and (10):

$$k_1 = 0$$
$$k_2 = 5.41 \times 10^{-3}/P_r \text{ sec}^2$$
$$k_3 = 7.36 \times 10^{-3}/P_r \text{ sec}^2$$
$$k_4 = 7.85 \times 10^{-4}/P_r$$
$$k_5 = k_8 = 0$$
$$k_7 = 1.02 \times 10^{-2}/P_r$$

$$H_1 = 3.44$$
$$H_2 = 0.39$$
$$H_3 = 3.21$$
$$H_4 = 0.03$$

The value of the effective back pressure, P_d (see Eq. (15)) is obtained empirically as is discussed in subsequent paragraphs.

a. Pressure and displacement variations with time.

Figures 9-12 show the results of the analog computer solutions to the analytical model for the conditions under consideration. The value of P_d, the effective back pressure, was set at 46psi except for the P_r = 50psi run (Fig. 9) where it was necessary to set P_d = 41psi. The logic of these selections is discussed in a subsequent section. In obtaining the fit of the analytical model to the data, as was done in Figs. 9-12, it was necessary to partition P_d into portions acting across the injector piston and across the slug. That is,

$$P_d = \frac{F_p}{A_i} + \frac{F_s}{A_c} + P_b = P_{di} + P_{ds}$$

$$\text{where } P_{di} = \frac{F_p}{A_i} \text{ and } P_{ds} = \frac{F_s}{A_c} + P_b.$$

In the four cases illustrated, it was found that the static drag was almost entirely due to the injector piston. The semi-empirical results are as follows:

Figure	P_r	P_d	P_{di}	P_{ds}
9	50	41	31	10
10	100	46	41	5
11	140	46	43	3
12	210	46	46	0

This information is of obvious use in pointing out the area to seek reductions in P_d.

The agreement of the analysis with the experimental measurements shown in Figs. 9-12 is remarkably good when it is realized that (1)

the step input assumed in the model is only crudely approximated by the experimental system and, (2), the model does not include compressibility effects. The latter discrepancy is believed to be the reason that the analytical model does not accurately follow the observed chamber pressure oscillations. These oscillations, caused by the accordion-like motion of the liquid between the injector piston and the slug, require the accounting for compressibility effects in the liquid. A careful examination of these results has shown that the deviations from the analytical model are also present in the displacement trace, although this is not obvious in the figures. The effect of the non-constancy of driving pressure, P_r, is partially removed by the semi-empiricism present in the selection of P_{id} and P_{sd}, as discussed above. Finally, it should be noted that the cases presented in Figs. 9-12 are randomly selected from a large number of runs. The entire body of original data is available upon request.

b. Ram-time variations with driving pressure.

Equation (14) gives a predicted ram-time dependency based upon a number of simplifying assumptions. Repeating the expression here,

$$t_f = \frac{1}{B'} \cosh^{-1} \exp\left(\frac{1}{A}\right)$$

where

$$\frac{1}{B'} = \left(\frac{2m_s D_c}{P_r A_c}\right)^{1/2} \frac{1 + H_1}{\left\{\left(\frac{c}{m_s}\right) H_3 \left[\left(\frac{D_r}{D_i}\right)^2 - \frac{P_d}{P_r}\right]\right\}^{1/2}}$$

and

$$A = \frac{k_2 (1 + H_1)}{k_3 H_3}$$

With the experimental conditions previously described, we have

$$\frac{1}{B'} = \frac{.156}{(P_r - P_d)}^{1/2} \quad \text{and}$$

$$A = 1.017$$

with the result that

$$t_f = \frac{256}{(P_r - P_d)}^{1/2} \quad \text{(msec)}$$

The agreement of this expression with the experimental data is shown in Fig. 14. To obtain this agreement, it has been necessary to account for the approximately 8 millisecond delay that is observed in the experiments. In addition, it is seen that a good estimate of P_d, for the system used, is 46psi. This remarkable agreement indicates the essential correctness of the model when used within the limits imposed by the assumptions. The main uncertainty in the model is about ±10% in the value of H_3. This uncertainty is equivalent to about ±2% in t_f.

5. General observations. The analytical model is seen to be well supported by the experimental data. It is therefore reasonable to utilize the analytical model to extrapolate the experimental results to cases of special interest. In particular, the analysis can be used to indicate the areas of redesign likely to be most profitable and to obtain preliminary predictions of LPG loading system performance under a variety of design conditions obtained through the specification of values of parameters different from those analyzed to date. These parameters include caliber size, charge-to-mass ratio, and projectile mass (or propellant density). Results of such parametric studies are

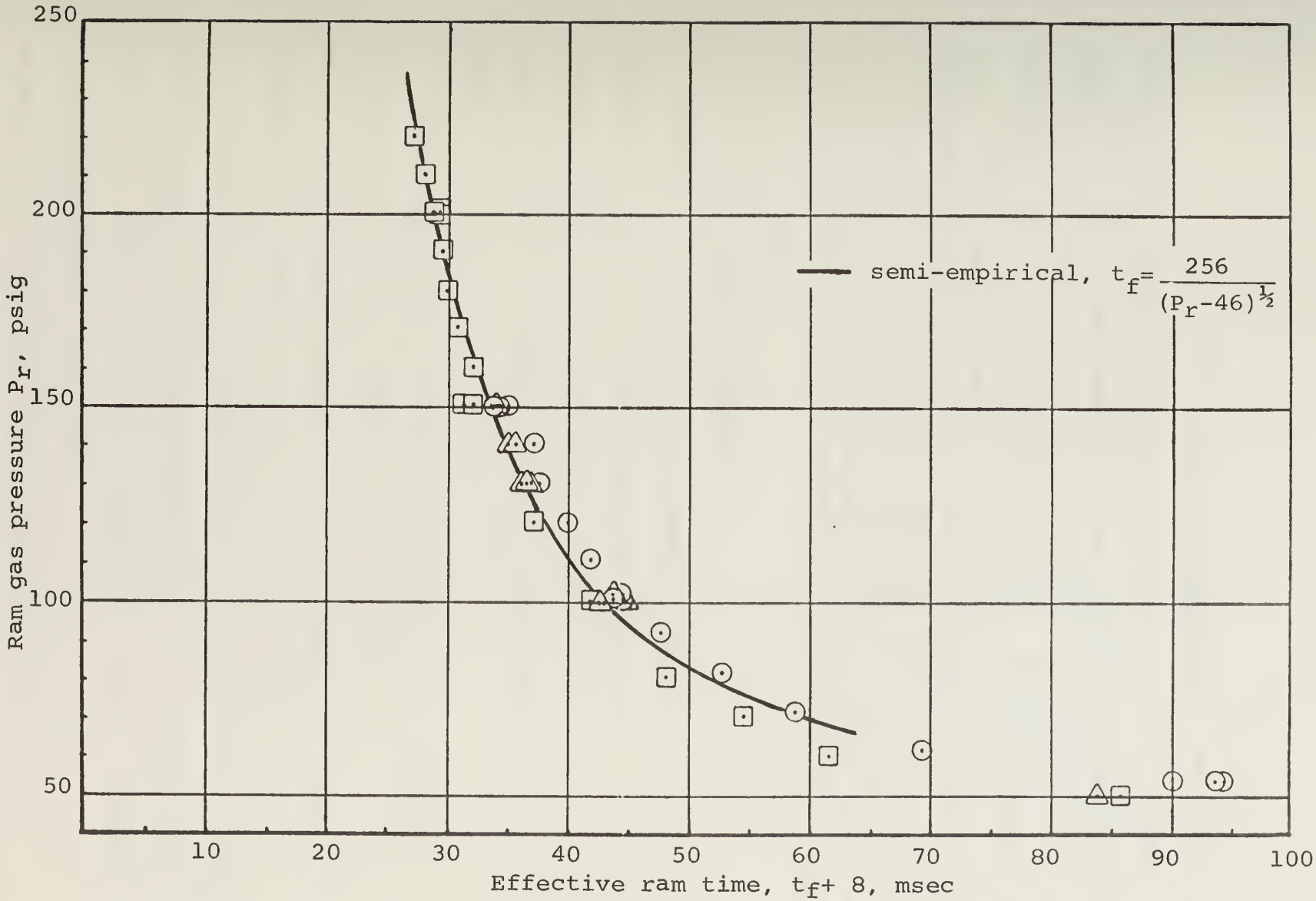

Figure 14. Ram time vs ram gas pressure; comparison with theory.

reported in the following section.

Finally, it should be pointed out that, as expected, the analytical model only partially predicts the instantaneous behavior of the liquid and solid masses during loading. If knowledge of the mean behavior with respect to time is insufficient information, it is imperative that the model be expanded to take the driving system (compressed gas) into account and to allow for compressibility effects in the liquid. Some further comments on this subject are offered at the conclusion of the report.

IV. DESIGN CONSIDERATIONS

In this section the analytical model is utilized to demonstrate those design decisions that are most influential in determining the performance of LPG propellant loading systems. For the purposes of the following remarks, "performance" is taken to mean ram-time. Other criteria (such as chamber pressure levels and system volume) are also amenable to prediction by the analytical model but ram-time is considered here due to its wide acceptance as a quantity to be minimized in any LPG system.

A. REDESIGN OF THE LPG SIMULATOR

Appendix D describes the analog computer program that has been developed to solve the governing equations (9) and (10). This program has been used to predict the behavior of the existing laboratory system and to point the way toward the most profitable areas for redesign emphasis.

Figures 15a-e show the computer outputs for slug displacement, velocity, acceleration, chamber pressure, and slug pressure, respectively, for a range of reservoir pressures from 100 to 250psig. The values of the parameters are those presented previously in Section III.C.4 of this report. The parameters k_2 and k_3 are mainly dependent upon operational specifications (slug mass, caliber, charge-to-mass ratio, etc.) and are therefore not suitable for redesign. The other k_i parameters are negligibly small in the existing system. The parameters H_1 and H_3, representing inertia and viscous effects, respectively, are representative of two central areas for redesign.

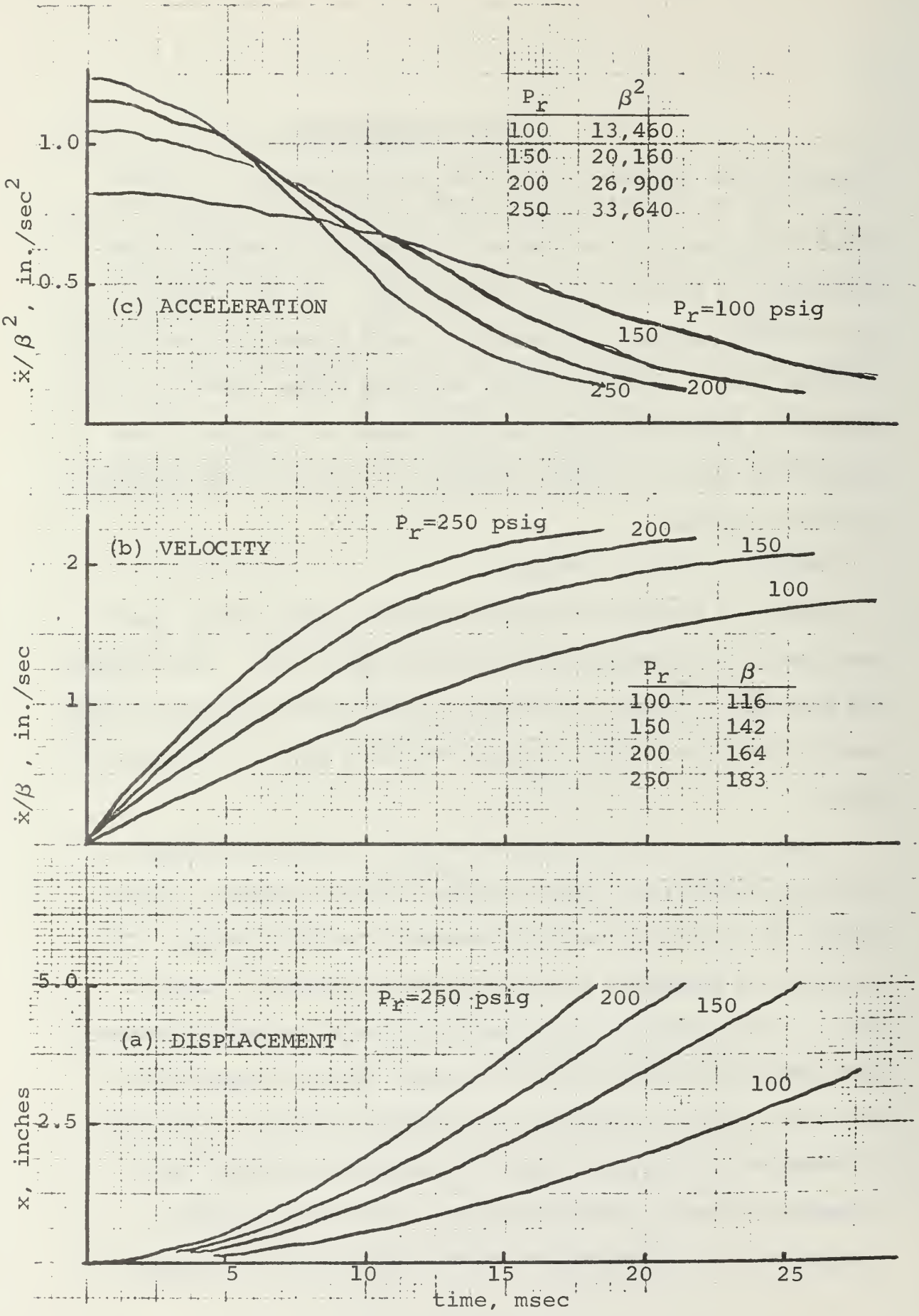

Figure 15. LPG simulator, analog solutions.

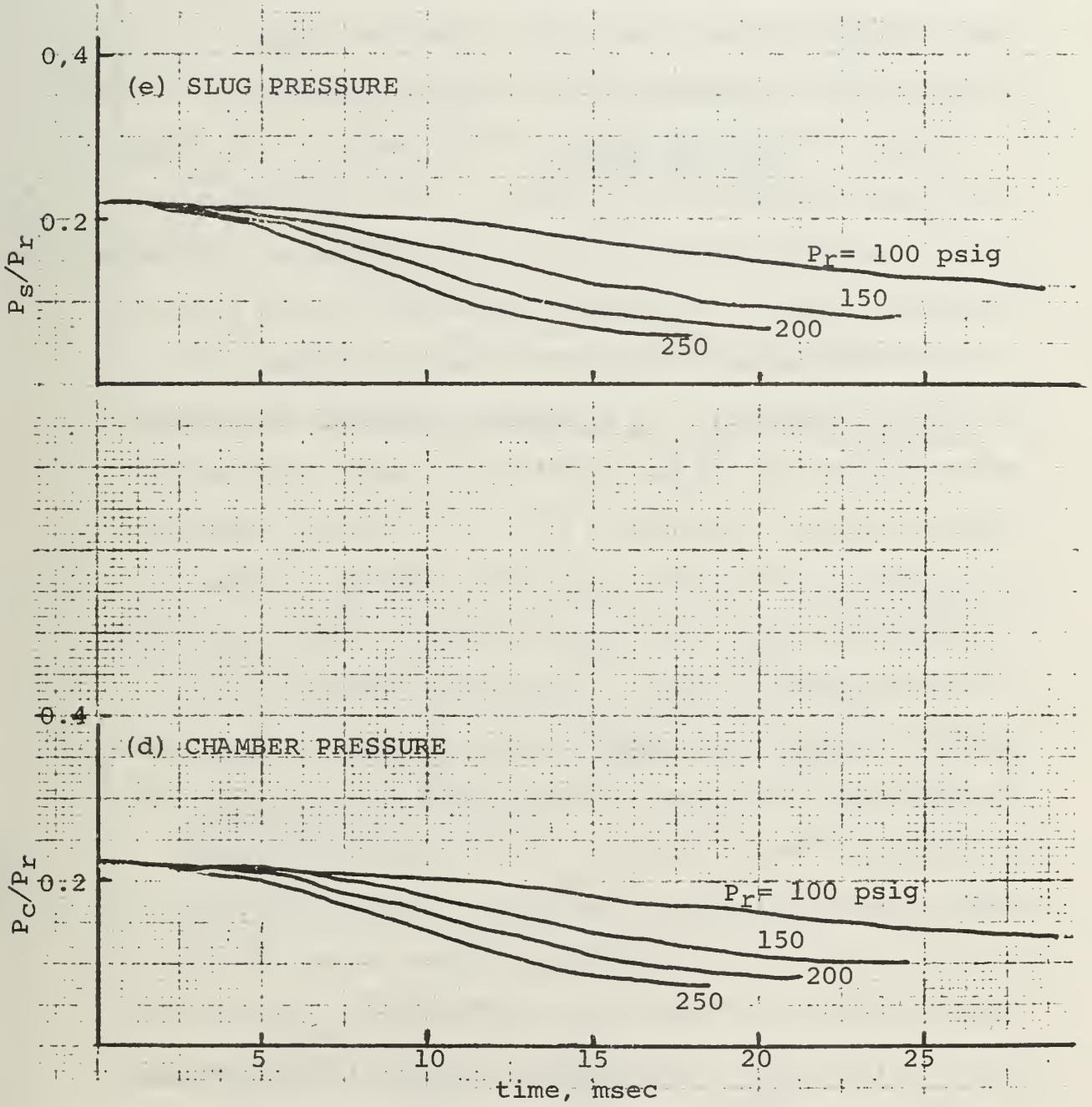

Figure 15 (concluded).

With H_1 = 3.44 and H_3 = 3.21, we see from Eq. (20) that R = 1.42 and the system is therefore inertia dominated from a ram-time point of view. The third parameter that might be improved is the static drag on the system, represented by the effective back pressure P_d.

Figures 16a-c show the effects of the parameters H_1, H_3, and P_d at a reservoir pressure of P_r = 150psig. Each of these parameters have been swept through four-fold reductions from the existing design. From these figures it is seen that ram-time decreases of 3.5, 5.5, and 2.5 milliseconds are predicted for four-fold decreases in P_d, H_1, and H_3, respectively. It is apparent, therefore, that redesign priorities should be inertia reduction (H_1), static drag reduction (P_d), and viscous loss reduction (H_3), in this order. Inspection of the parameters H_1 and H_3 will show that a reduction in connecting line length (L_ℓ) and/or an increased connecting line diameter (D_ℓ) will decrease both H_1 and H_3. A significant reduction in H_1 is attainable through the decrease of piston mass (m_p) or the increase of injector area (this term is already rather small, however, relative to the third term in H_1). H_3 can be significantly reduced mainly through shortening of line length, increasing the line diameter, and, most importantly, reduction of minor losses. In the current system, minor losses make up about 85% of H_3 (thereby pointing up a discrepancy in terminology). The effective back pressure is apparently due mainly to drag at the injector end of the system. This term is also influenced (due to inadequacies of modeling of the input pressure) by a non-constant reservoir pressure.

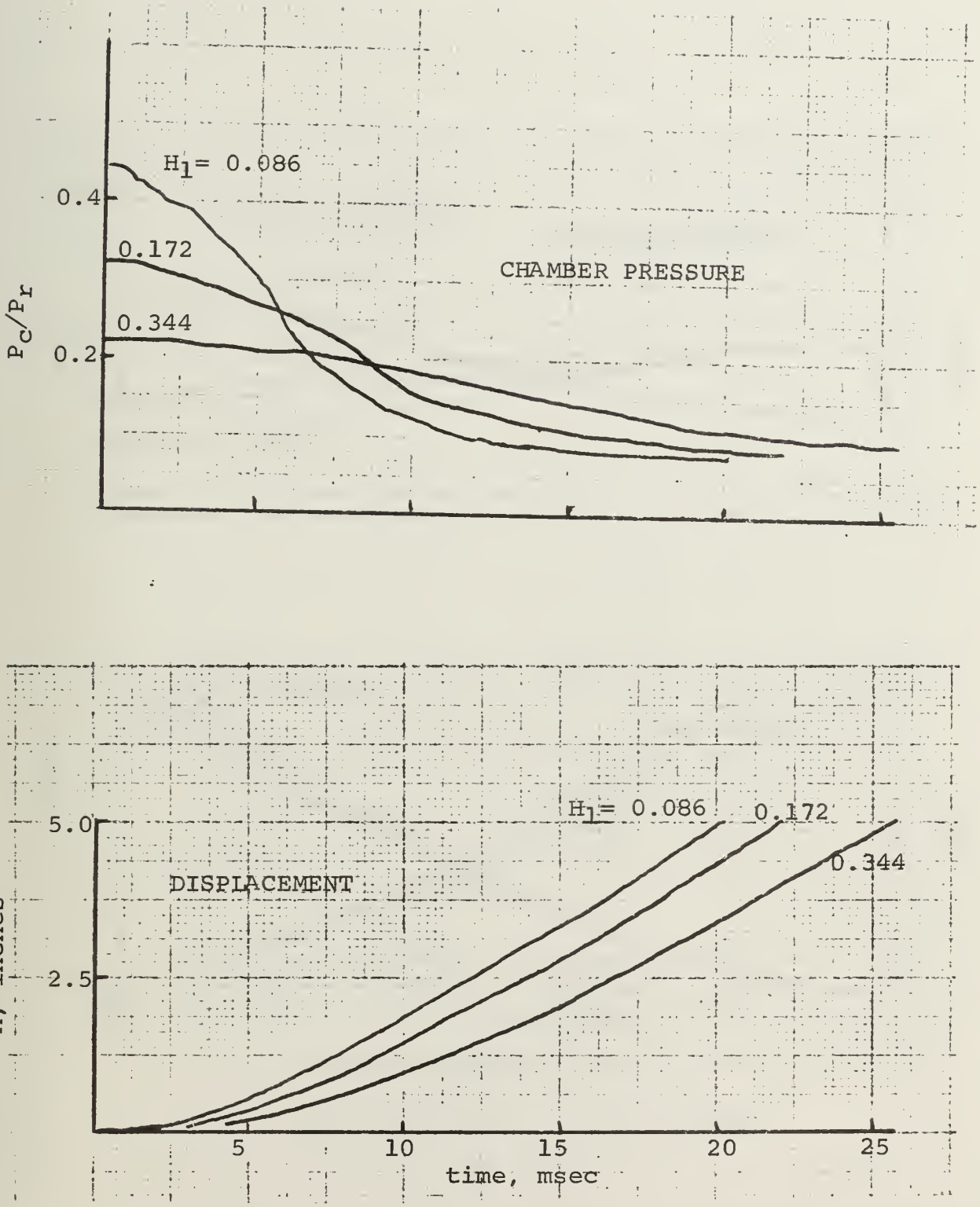

Figure 16(a). H_1 sweep, P_r= 150.

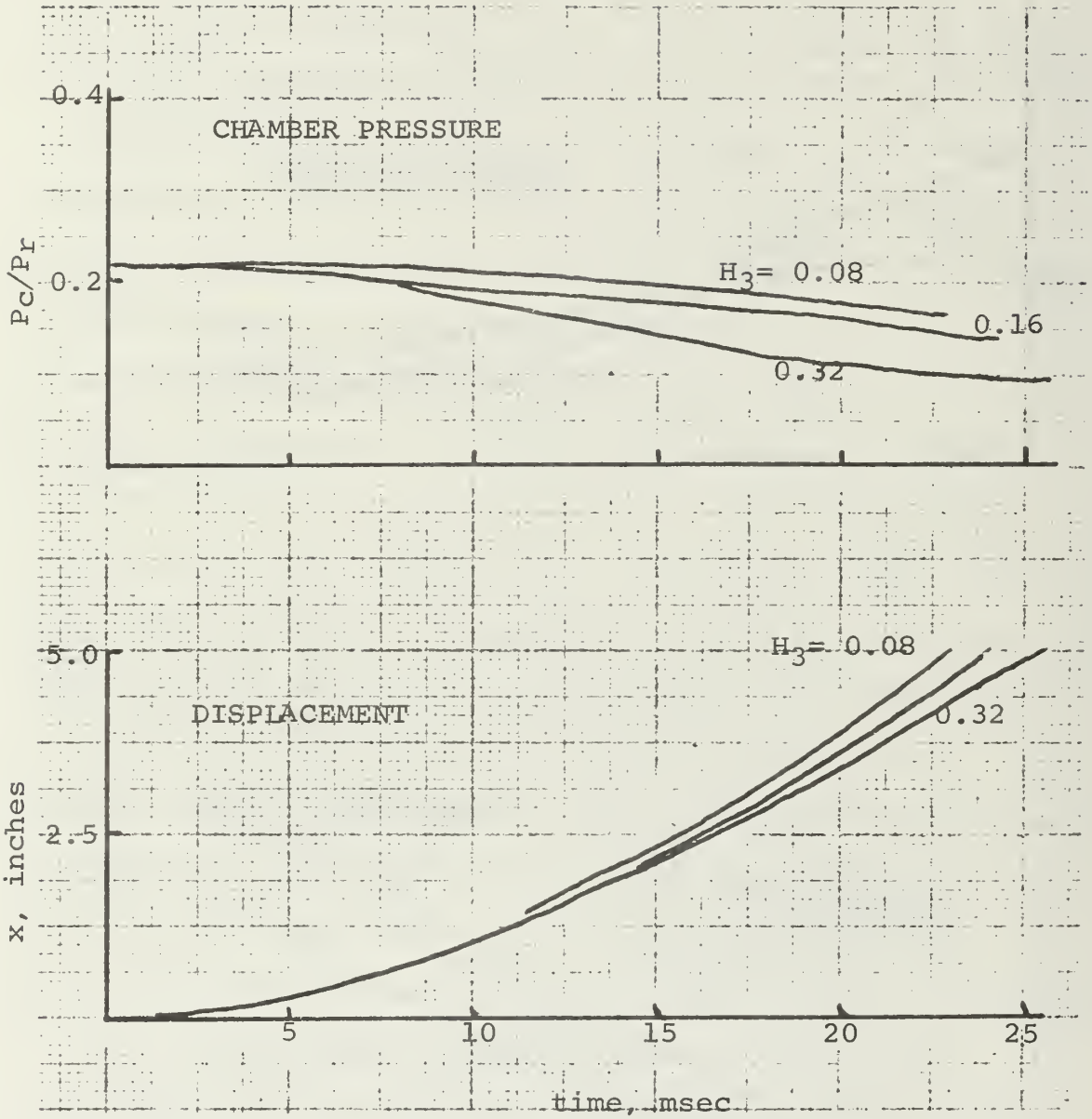

Figure 16(b). H_3 sweep, P_r= 150.

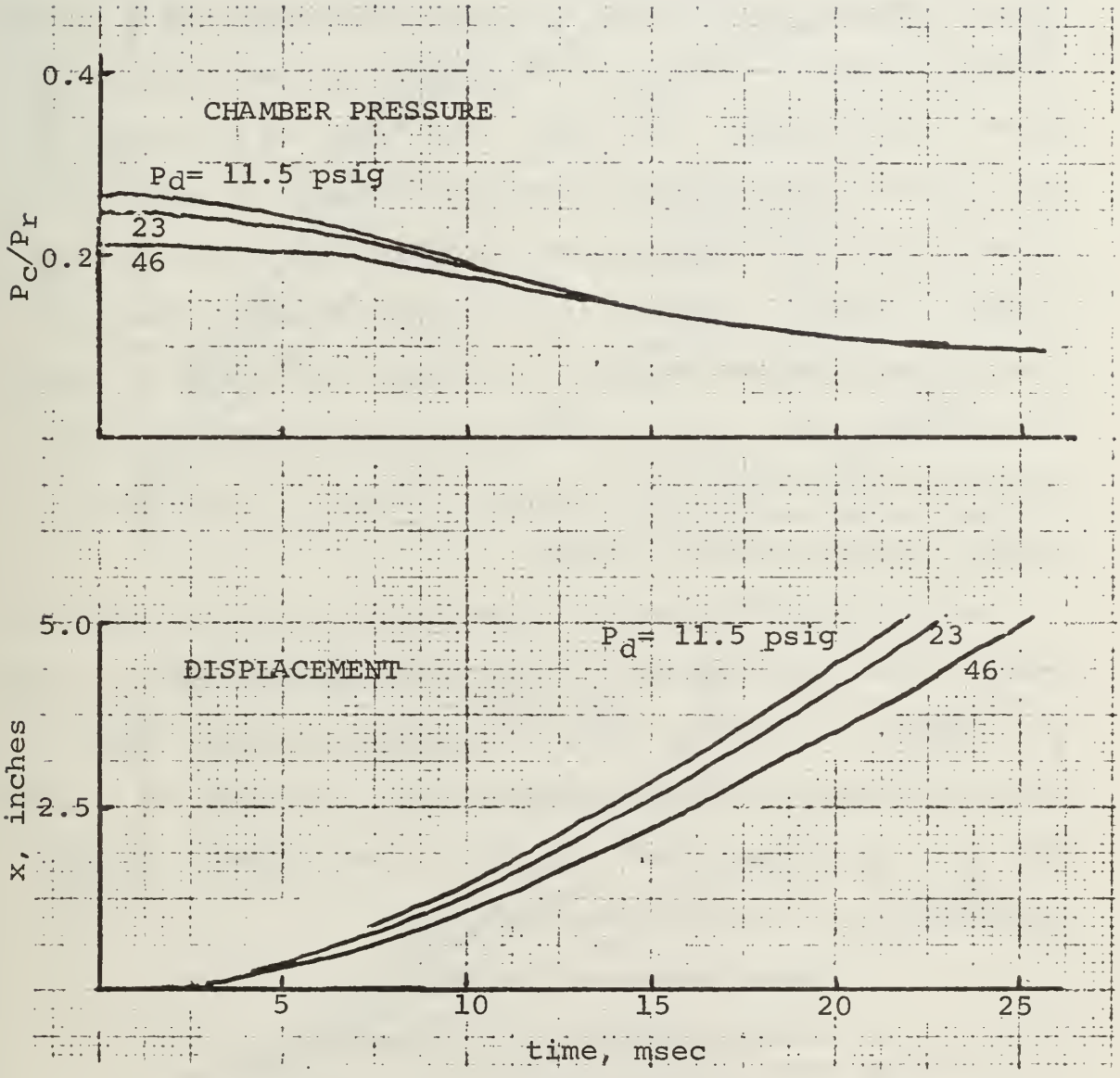

Figure 16(c). P_d sweep, P_r= 150.

Figures 17a-e show predicted performance curves calculated by assuming a two-fold reduction in all of the redesign parameters. That is, in these calculations, P_d = 23psig, H_1 = 1.72, and H_3 = 1.60. Referring to the P_r = 150psig curve, we see a ram-time reduction of about 7.5 milliseconds. This appears to be about one millesecond more than that calculated by simply adding the separate reductions observed in Fig. 16 (thus, the non-linearity of the problem is manifested). Figure 17 shows that if the two-fold parameter reductions are attainable through redesign, a ram-time of 15 milliseconds should be attainable with a reservoir pressure of about 200psig. Allotting 25% of the total firing cycle to liquid loading, this would permit a rate of fire 1000 rounds per minute.

In concluding this section, it should be noted that all delays in loading, other than those due to actual motion of the injector, liquid, and slug,have been omitted from this discussion. The 8 millisecond static delay observed in our experiments would, of course, be unacceptable in an operational system. With this caveat, however, redesign recommendations, in order of importance, are:

1. Reduce connecting line length.
2. Increase connecting line diameter.
3. Decrease piston mass and static drag.
4. Seek out and reduce minor losses.

B. PRELIMINARY DESIGN OF A 5-INCH SYSTEM.

In this section, the analytical model is exercised in order to demonstrate its utility in making first-cut design decisions applicable

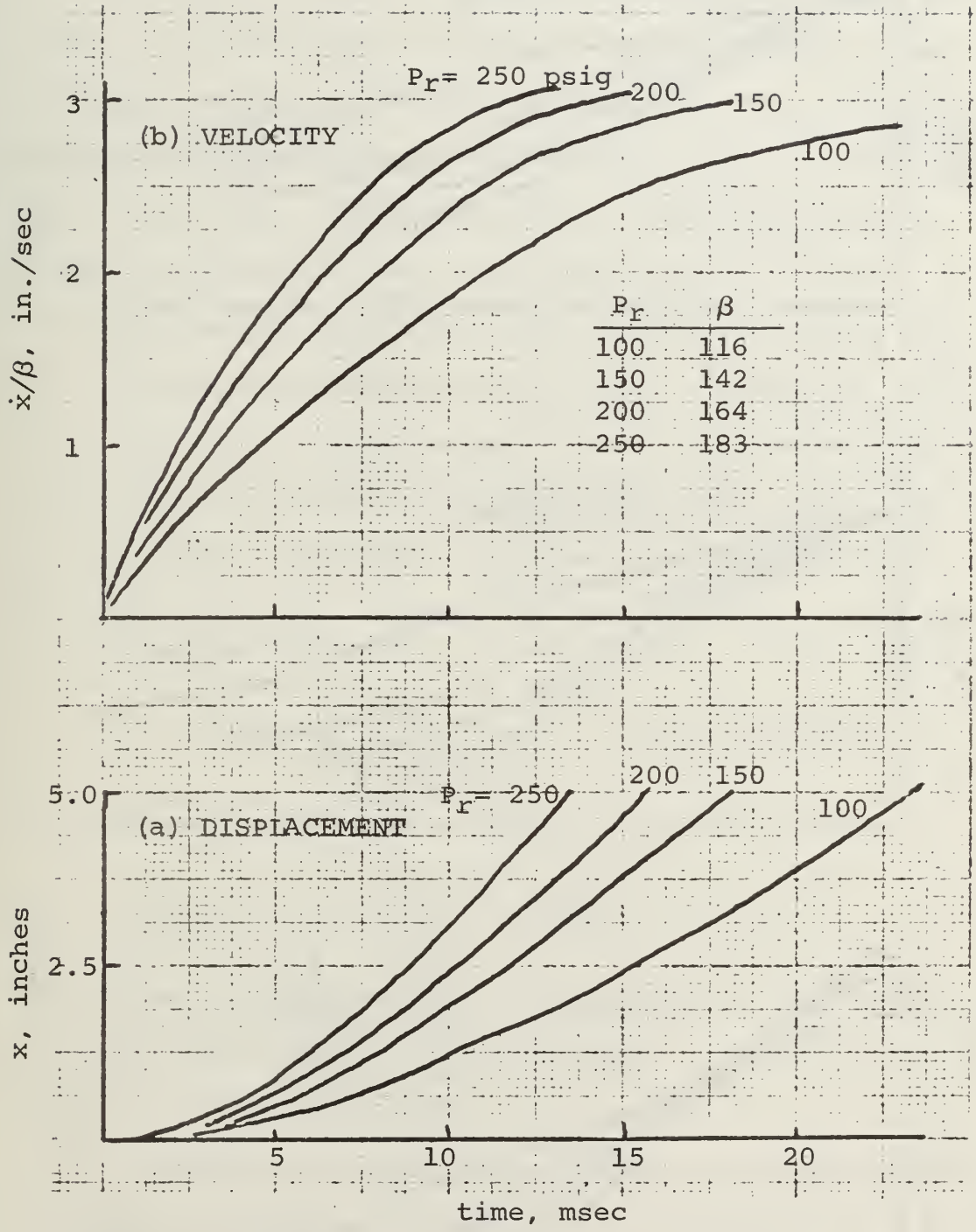

Figure 17. Predicted performance, LPG redesign.

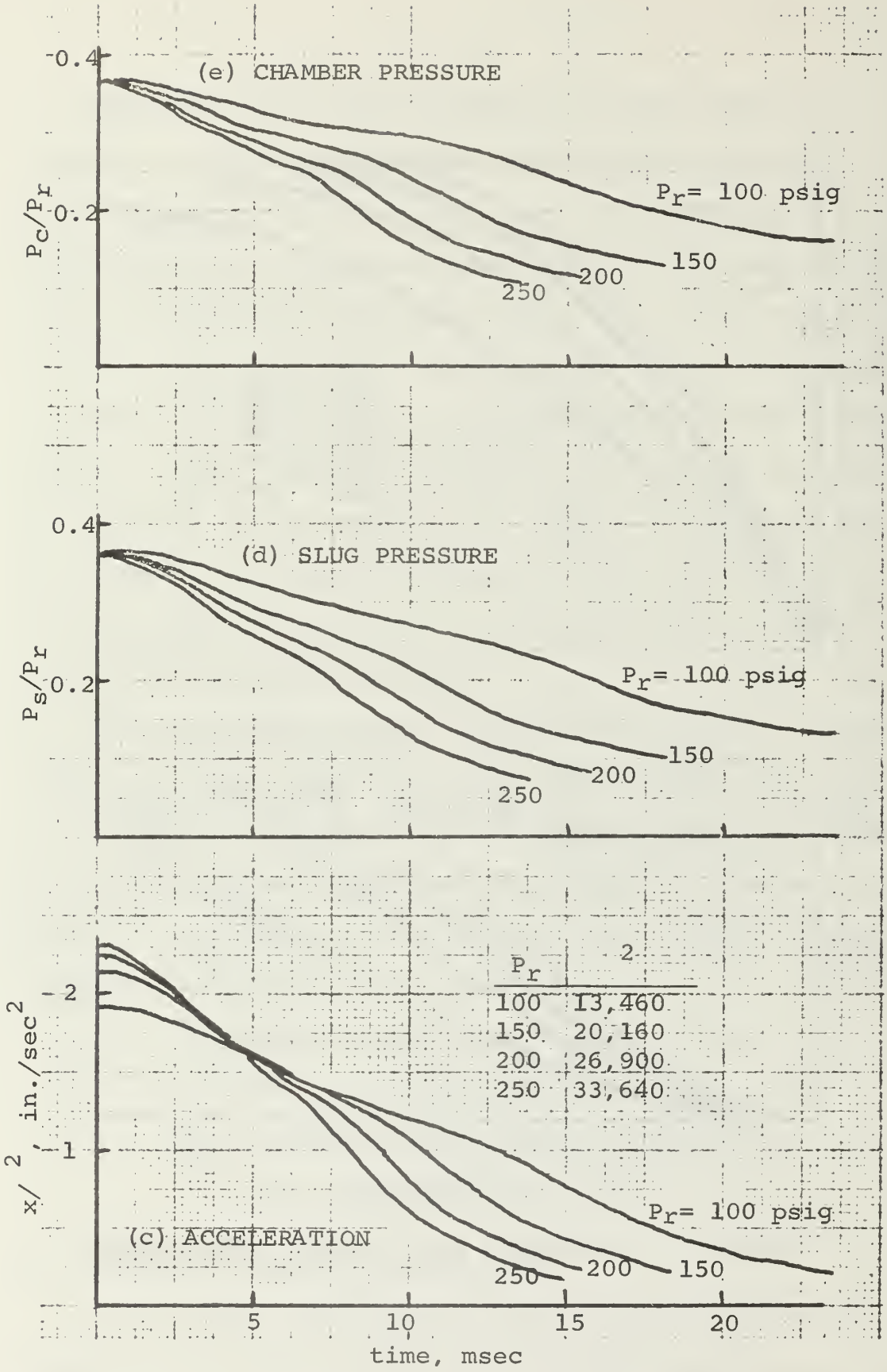

Figure 17 (concluded).

to liquid loading systems for guns of different scale. Before proceeding, it is noted, once and for all, that the validity of these predictions is vitally dependent on the extent to which the basic analytical model approximates the system under design. In particular, any current injector design will probably require a more complex mathematical description than that given by Eqs. (1) and (2).

For the purposes of this discussion, we shall rely mainly upon Eq. (14) which describes the semi-linear case in which H_4/H_3, $H_2/(1+H_1)$, and (k_5+k_8) are all negligibly small. These are desirable design constraints and are relatively easily obtained. In any case, in sections II.A.2.a. and b., the effects of departures from these conditions have been shown to be small. Repeating Eq. (14) in a slightly reworked form

$$t_f = \left[\frac{k_3 H_3}{\left(\frac{D_r}{D_i}\right)^2 - \frac{P_d}{P_r}} \right]^{1/2} A \cosh^{-1} \exp (1/A) \qquad (23)$$

$$\text{where} \quad A = \frac{k_2(1 + H_1)}{k_3 H_3} = R^2/2$$

Note the physical interpretation of the parameter A: it is a measure of inertia effects relative to viscous effects. The function of A in Eq. (23) is shown in Fig. 18.

It is now necessary to postulate a few design parameters descriptive of a 5-inch baseline LPG propellant loading system. It is to be emphasized that this baseline design need only be approximate since it is the function of the model to point up profitable departures from the baseline. For this example, the baseline system is

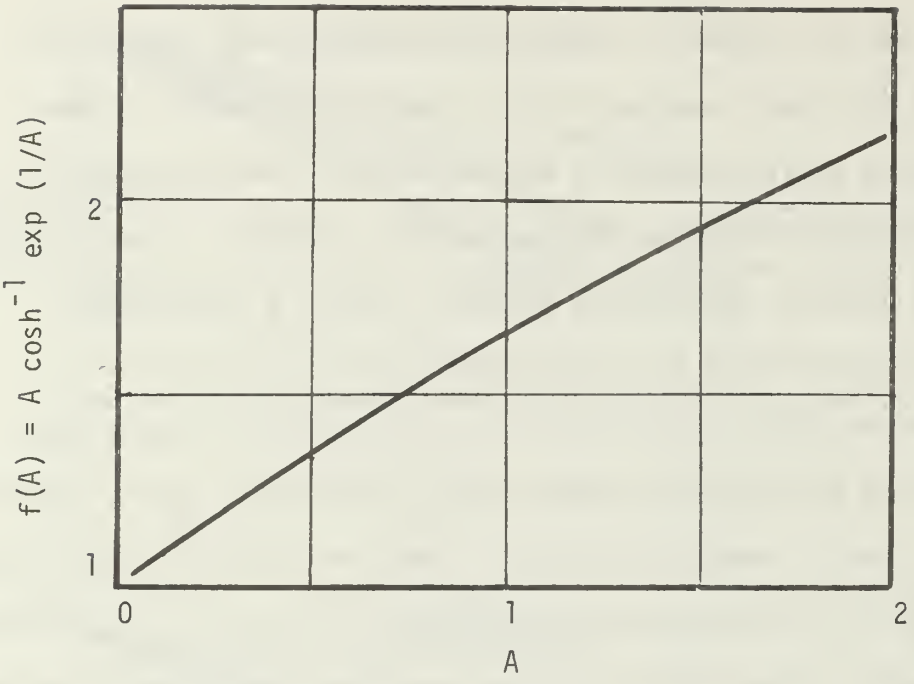

Figure 18.

described as follows:

Chamber diameter	$D_c = 5.0$ in.
Charge-to-mass ratio	$c/m_s = 0.5$
Propellant density	$\rho = 1.3 \times 10^{-4}$ lb sec^2/in.^{4}
Slug mass	$m_s = 80$ lb$_m$ = 0.207 lb sec^2/in.
Driving pressure	$P_r = 250$ psig

$\frac{m_p}{m_s} = 1.0$, $\frac{P_d}{P_r} = 0.1$, $n = 2$

$\frac{D_c}{D_i} = 0.5$, $\frac{D_c}{D_\ell} = 5.0$, $\frac{D_r}{D_i} = 1.0$,

$\frac{L_i}{x_{sm}} = 1.0$, $\frac{L_\ell}{x_{sm}} = 1.0$, $\sum_i k_{mi} = 20$

The length of slug travel can be calculated from

$$x_{sm} = \frac{m_s(c/m_s)}{\rho A_c} = 40.6 \text{ in.}$$

The pertinent parameters are found to be

$$k_2 = 1.71 \times 10^{-3} \text{ sec}^2$$

$$k_3 = 3.47 \times 10^{-3} \text{ sec}^2$$

$$H_1 = .0625 + .125 + 6.25 = 6.44$$

$$H_3 = .0009 + 23.44 + 2.46 = 25.90$$

Note the dominance of the connecting line contributions, 6.25 and 23.44, to H_1 and H_3, respectively. From these values, we calculate

$$A = 0.141 \text{ and } R = 0.53$$

so that this design is seen to be dominated by viscous effects. From Fig. 18, f(A) = 1.1 and the ram time is $t_f = 0.35$ sec. With the criterion of 25% of the total cycle time available for liquid loading, this baseline ram-time will allow a rate-of-fire of about 43 rounds-per-minute.

There is a limitless number of perturbations on the baseline design that can be performed in order to examine their effect upon rate-of-fire. Judicious choice of these perturbations awaits the specification of more exact performance and design criteria. As examples of what can be done, however, it is noted that this particular baseline design is severely constrained by inertia and viscous losses in the connecting lines between injector and breech. Thus, if the number of 1-inch connecting lines is doubled (to n = 4), we calculate $H_1 = 3.31$, and $H_3 = 8.32$, so that A = 0.255 and $R = 0.714$. The resulting maximum rate-of-fire is about 71 rounds-per-minute, a 65% improvement. As another example, if the injector diameter is constrained so that $D_c/D_i = 1.0$, the resulting rate-of-fire, for the n = 4 case, is about 55 rounds-per-minute, a 29% decrease.

As a final demonstration of the analytical capability thus far developed, the baseline 5-inch design has been modeled on the analog computer for various driving pressure levels. The results are shown in Figs. 19a-e.

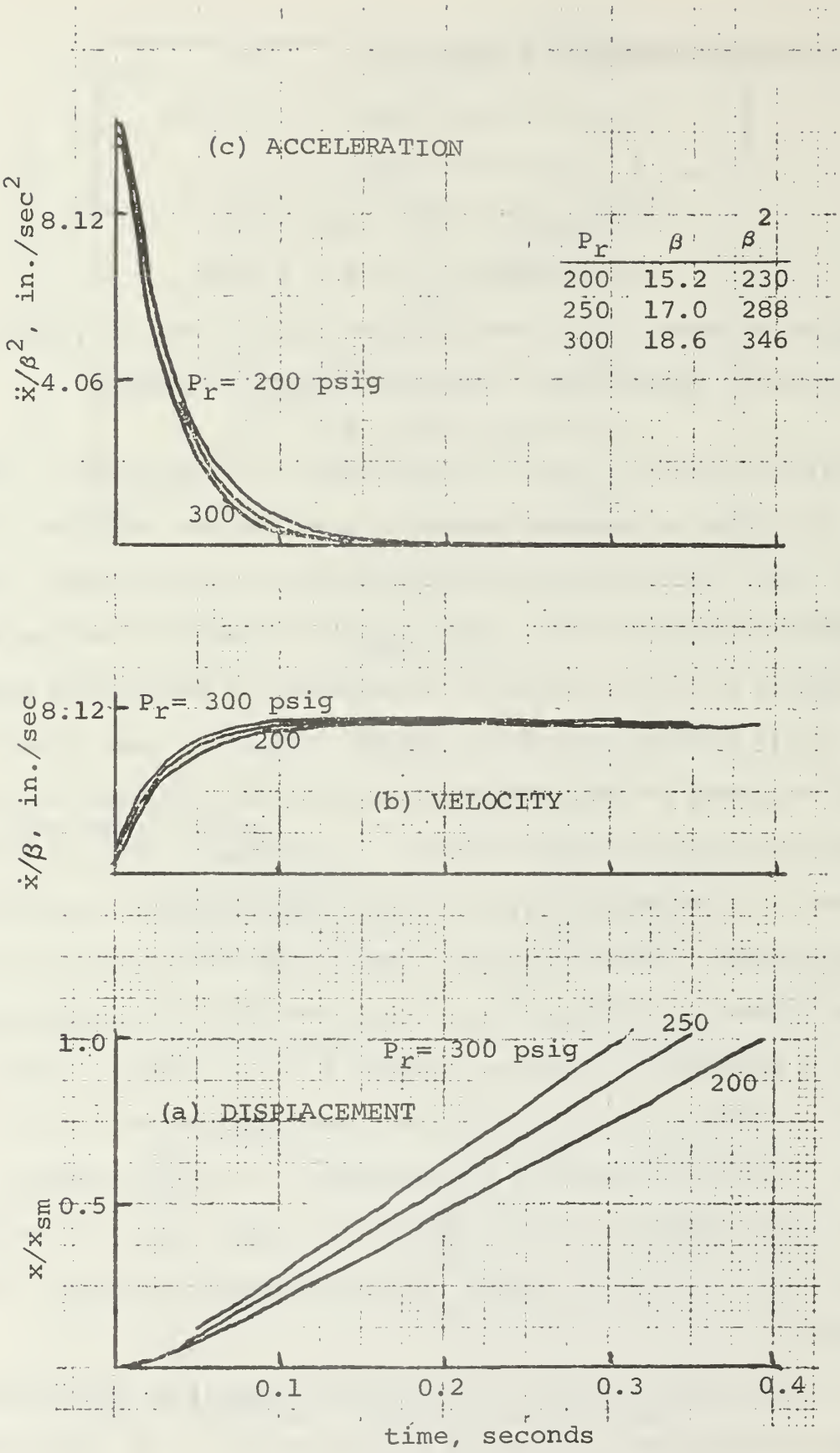

Figure 19. Predicted performance of 5-inch baseline design.

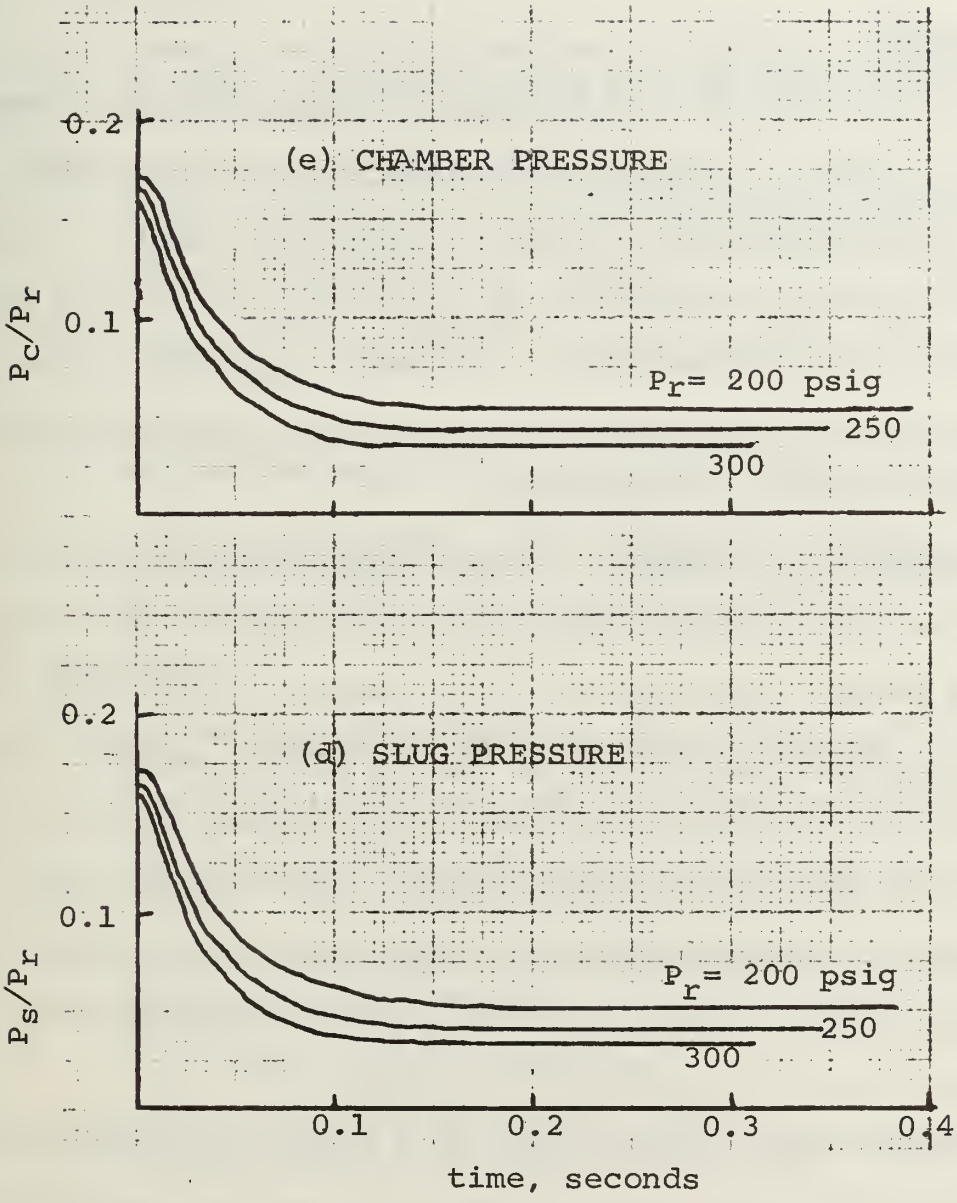

Figure 19 (concluded).

V. SUMMARY

A. CONCLUSIONS

An analytical model has been developed to predict the time-dependent behavior of the moving liquid and solid masses during an LPG loading cycle. This model has been tested against experimental results obtained with an LPG laboratory simulator and has been found to be adequate for the prediction of system performance. The model is specifically constrained in its use by the assumption of an incompressible liquid and a uniform step input in driving pressure.

An experimental LPG simulator has been designed and fabricated to assist in verifying analytical predictions and to identify design and performance phenomena requiring particular attention in future LPG developments. Measurements made with the LPG simulator, together with guidance provided by the analytical model, have provided valuable insights into the behavior to be expected from a given LPG feed system design. Specific unanswered questions relate to the effects of large trapped gas volumes and the existence and probable effects of cavitation in the liquid slug during the loading cycle.

The analytical model has been shown to be useful in the prediction of the influence of design specifications such as caliber, projectile mass, charge-to-mass ratio, propellant properties, and system geometry and scale. It is anticipated that the analysis, further substantiated by experimental observation and improved as required for future application, will provide a valuable tool in the design of prototype and operational LPG systems.

B. RECOMMENDATIONS

1. Experimental

a. Incorporate design improvements as suggested by the analytical model. Test the modified LPG simulator to verify the expected performance increases.

b. Conduct tests to verify other parametric dependencies predicted by the model. Those most easily evaluated include propellant properties (simulate a liquid propellant), charge-to-mass ratio, and slug mass.

c. Investigate the effects of large volumes (up to 10%) of ullage gas.

d. Determine the existence of cavitation and, if it is found, evaluate the effect of cavitation upon system performance.

e. Develop the simulator to the point that it can be operated in the fully automatic mode. Conduct tests appropriate for the evaluation of the system in this mode.

2. Analytical

a. Continue to refine the model. The difficulty of including compressibility effects may preclude this improvement unless future requirements justify the necessary effort.

b. Program the governing equations for solution on the digital computer. This will be necessary if the model is extended.

c. Model upstream driving systems in order to obtain accurate inputs to the existing model. This will be necessary if the analysis is to provide performance predictions for the fully automatic mode of operation.

d. Monitor LPG program developments with a view to subjecting emerging designs to evaluation by the model.

VI. REFERENCES

1. Experiment, Inc., Richmond, Va., Liquid Fuel Catapult, TP31, Contract W-36-034-ORD-7661, November 1947.

2. Experiment, Inc., Richmond, Va., Liquid Fuel Catapult, II, Further Investigations at Caliber .50 Scale, TP33, Contract W-36-034-ORD-7661, August 1948.

3. Experiment, Inc., Richmond, Va., Liquid Fuel Catapults with Regenerative Injection, I, Design and Test of Preliminary Caliber .50 Models, TP38, contract W-36-034-ORD-7661, December 1949.

4. Experiment, Inc., Richmond, Va., Liquid Fuel Catapult, IV, Miscellaneous Studies with Caliber .50 Systems, TP40, Contract W-36-034-ORD-7661, September 1950.

5. Experiment, Inc., Richmond, Va., Liquid Fuel Catapults with Regenerative Injection, II, The Design of a 37mm Launcher, TP39, Contract W-36-034-ORD-7661, December 1949.

6. Experiment, Inc., Richmond, Va., Liquid Fuel Catapults with Regenerative Injection, III, Design Improvements and 37mm Test Results, TP41, Contract W-36-034-ORD-7661, December 1949.

7. Frankford Arsenal, Philadelphia, Pa., Symposium on Liquid Propellants for Guns, "Summary Research and Development of Liquid Propellant Guns," R-997, December 1950.

8. Naval Ammunition and Net Depot, Seal Beach, California, Design of an Experimental Liquid Propellant Injection System for a 40mm Gun, 20 July 1950.

9. Frankford Arsenal, Philadelphia, Pa., Symposium on Liquid Propellants for Guns, "The Limits of Gun Performance," R-997, December 1950, p. 46.

10. E. Justin Wilson, Jr., "Resume of Liquid Propellant Gun Activities at Experiment Incorporated," Proceedings of the 3rd Annual Conference on Liquid Propellant Guns, December 15, 1952, p. 137.

11. Experiment, Inc., Richmond, Va., Repetitively Firing Liquid Propellants for Small Arms, Final Report TP-88, January 1956.

12. Experiment, Inc., Richmond, Va., Application of Liquid Propellants to Guns and Launchers,III, p. 95, October 1955.

13. Detroit Controls Corporation, Liquid Propellant Gun Systems, RC-190, Final Summary Report, April 1, 1956.

14. Experiment, Inc., Richmond, Va., Liquid Propellants for Tank Guns, I, a Feasibility Study, Final Report, TP-70, April 1954.

15. Stanford Research Institute, Menlo Park, California, Survey of Problems in Developing Tank Cannon, Final Report on SRI Project P-902, March 1954.

16. Detroit Controls Corp., Redwood City, California, Investigation of Liquid Propellant Gun Systems for 90mm Tank Guns, Final Report, RC-224, January 1957.

17. Experiment, Inc., Richmond, Va., Design, Construction, and Test of Liquid Propellant Guns for Medium Tanks, TP-112, August 1957.

18. Quantic Industries, Inc., San Carlos, Calif., Investigation of Performance, Ignition, Safety, and Handling Characteristics of Liquid Propellants for Application to Liquid Propellant Guns, Final Report A-WTD-106, December 1968.

19. General Electric Company, Armament Department, Liquid Propellant Gun Study, Final Report, 70APB580, October 1970.

20. Pulsepower Systems, Inc., San Carlos, Calif., Investigation of Liquid Propellant Gun Systems Employing Improved Propellant, Final Report TR-19, August 1970.

21. National Bureau of Standards, Handbook of Mathematical Functions, ed. M. Abramowitz and I. A. Stegun, U. S. Government Printing Office, Washington, D.C., March 1965, p. 319.

22. Gibson, E. J., "Experimental Investigation of the Fluid Dynamic Characteristics of Liquid Propellant Gun Loading Systems," M.S. Thesis, Naval Postgraduate School, Monterey, CA, March 1975.

APPENDIX A

NOMENCLATURE

a	parameter defined in conjunction with Eq. (16).
A	cross-sectional area
C_c	contraction coefficient
C_d	discharge coefficient
(c/m_s)	charge-to-mass ratio
D	diameter
f	fluid friction factor
F	static drag force
$H_1..H_4$	parameters defined in conjunction with Eqs. (9) and (10)
k_f	damping force coefficient
k_s	spring force coefficient
k_m	minor loss coefficient
$k_1..k_9$	parameters defined in conjunction with Eqs. (9) and (10)
L	length
m	mass
n	number of connecting lines
P	pressure
P_b	back pressure on slug
P_d	effective back pressure defined in conjunction with Eq. (15)
R	ratio defined in Eq. (20)
t	time
t_f	final time, ram-time

x	displacement, position
x_{sm}	final slug displacement
β_e	effective bulk modulus
ζ	damping factor
ρ	liquid density
ω_n	natural frequency, radians/second

Subscripts

c	refers to chamber
i	refers to low pressure (liquid) side of injector; also counting index
ℓ	refers to connecting line(s)
p	refers to injector piston
r	refers to high pressure (reservoir) side of injector
s	refers to slug

APPENDIX B

CLOSED FORM SOLUTIONS TO THE GOVERNING DIFFERENTIAL EQUATION

We seek solutions to the equation

$$k_2\ddot{x}(1 + H_1 + H_2 x) + k_3\dot{x}^2(H_3 + H_4x) + (k_4+k_7)\dot{x} + (x_5 + k_8)x = a \qquad (B1)$$

$$\dot{x}(o) = x(o) = o$$

1. Semi-linear

Let $\frac{H_4}{H_3} << 1$, $\frac{H_2}{1+H_1} << 1$, $k_5 + k_8 << 1$, so that

$$k_2 (1 + H_1) \ddot{x} + k_3H_3\dot{x}^2 + (k_4 + k_7) \dot{x} = a$$

Let $z = \dot{x}$, then $k_2(1 + H_1) \dot{z} + k_3H_3z^2 + (k_4 + k_7) z = a$, and

$$\frac{dz}{a - (k_4 + k_7)z - k_3H_3z^2} = \frac{dt}{k_2(1 + H_1)}$$

and, after integration and application of the limits

$$\frac{-2}{\sqrt{q}} \tanh^{-1}\left[\frac{-2k_3H_3z - (k_4 + k_7)}{\sqrt{q}}\right] + \frac{2}{\sqrt{q}} \tanh^{-1}\frac{-(k_4+k_7)}{\sqrt{q}}$$

$$= \frac{t}{k_2(1 + H_1)}$$

where $q = (k_4 + k_7)^2 + 4ak_3H_3$

Upon rearrangement and solution for $z = \dot{x}$, we have

$$\dot{x} = AB \tanh B(t + t_o) - C \qquad (13)$$

where the constants are defined in the main body of the report. Expressions for $x(t)$ and $\ddot{x}(t)$ are obtained through integration and differentiation of this expression.

2. Inertia effects only. Equation (B1) becomes

$$k_2 \ddot{x} (1 + H_1 + H_2 x) = a \qquad (B2)$$

Multiplying by $2\dot{x}$

$$2\dot{x}\ddot{x} = \frac{2\dot{x}a}{k_2(1 + H_1 + H_2 x)}$$

or

$$d(\dot{x}^2) = \frac{2a}{k_2} \frac{dx}{(1 + H_1 + H_2 x)}$$

so that

$$\dot{x} = \left[\frac{2a}{k_2 H_2} \ell n \left(1 + \frac{H_2 x}{1 + H_1}\right)\right]^{1/2} \qquad (B3)$$

Let $u = \left[\ell n \left(1 + \frac{H_2}{1 + H_1} x\right)\right]^{1/2}$ so that $dx = \frac{2(1 + H_1)}{H_2} u\, e^{u^2} du$

Equation (B3) becomes

$$\frac{2(1 + H_1)}{H_2} e^{u^2} du = \sqrt{\frac{2a}{k_2 H_2}}\, dt$$

or

$$\sqrt{\frac{k_2 H_2}{2a}} \left[2 \frac{(1 + H_1)}{H_2}\right] \int_o^u e^{z^2} dz = t$$

and, since $e^{-u^2} = \frac{1}{1 + \frac{H_2}{1 + H_1} x}$, upon rearranging,

$$t = \left(1 + \frac{H_2}{1 + H_1} x\right) \left[\frac{2k_2(1 + H_1)}{a} \left(\frac{1 + H_1}{H_2}\right)\right]^{1/2} D(u)$$

where $D(u) = e^{-u^2} \int_0^u e^{z^2} dz$ is Dawson's integral [21].

3. Fluid friction only. In this case, Eq. (B1) becomes

$$k_3 \dot{x}^2 (H_3 + H_4 x) = a$$

$$(H_3 + H_4 x)^{1/2} dx = \left(\frac{a}{k_3}\right)^{1/2} dt$$

and, upon integration and evaluation of the limits,

$$t = \frac{2}{3} \frac{H_3}{H_4} \left(\frac{k_3 H_3}{a}\right)^{1/2} \left[\left(1 + \frac{H_4}{H_3} x\right)^{3/2} - 1 \right]$$

Note that since we have reduced the order of the basic equation, the initial condition $\dot{x}(o) = o$ cannot be satisfied in this formulation.

APPENDIX C

NATURAL FREQUENCY AND DAMPING

The natural frequency, ω_n , and the damping coefficient, ζ , can be calculated by measuring the quantities indicated on the sketch below:

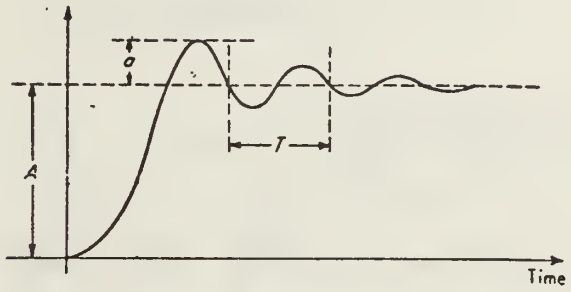

$$\zeta = \sqrt{\frac{1}{\left(\frac{\pi}{\ln[a/A]}\right)^2 + 1}}$$

$$\omega_n = \frac{2\pi}{T\sqrt{1 - \zeta^2}}$$

where ω_n is in rad/sec and T is in seconds.

A. Effective Bulk Modulus.

$$\omega_n^2 = \frac{A_p^2 \beta_e}{m_p V_t}$$

$$\beta_e = \frac{m_p V_t}{A_p^2} \omega_n^2$$

ω_n	natural frequency, rad/sec	(variable)
A_p	piston area, in^2	(1.767)
m_p	mass of piston, $\frac{lb\text{-}sec^2}{in}$	(5.2×10^{-3})
V_t	total volume of fluid, in^3	(21.389)
β_e	equivalent bulk modulus, psi	(variable)

The values in parentheses are for this experimental setup.

$$\beta_e = 0.0354\ \omega_n^2$$

B. Friction Factor, k_{fp}

$$\zeta = \frac{k_{fp}}{2A_p}\sqrt{\frac{V_t}{\beta_e m_p}}$$

$$k_{fp} = 2m_p\ \omega_n\ \zeta$$

$$k_{fp} = 0.01035\ \omega_n \zeta$$

C. Trapped Gas (Ullage).

$$\frac{1}{\beta_e} = \frac{1}{\beta_\ell} + \frac{1}{\beta_g}\ \frac{V_g}{V_t}$$

β_e	equivalent bulk modulus
β_ℓ	liquid bulk modulus
β_g	gas bulk modulus
V_g	total volume of gas in fluid

For a perfect gas $\beta_g \approx \gamma P$

where γ ratio of specific heats

P absolute pressure

For air at moderate to low pressures, it can be assumed that air approximates a perfect gas

$$\gamma_{air} = 1.4 , \quad \beta_g = 1.4P$$

$$\frac{V_g}{V_t} = \gamma P \left(\frac{\beta_\ell - \beta_e}{\beta_e \quad \beta_\ell} \right)$$

For water

$$\beta_\ell \approx 3 \times 10^5 \text{psi}$$

$$\frac{V_g}{V_t} = 1.4P \left(\frac{3 \times 10^5 - \beta_e}{3 \times 10^5 \beta_e} \right) \times 100\%$$

As previously reported in [22], the trapped gas volume thus calculated ranges from 0.1% to 0.5% of the total contained volume V_t.

APPENDIX D.

SOLUTION OF THE GENERAL GOVERNING EQUATIONS.

The governing equations, developed in Section II of this report, are repeated here:

$$1 - P_s = k_1 + k_2 \ddot{x}(H_1 + H_2 x) + k_3 \dot{x}^2 (H_3 + H_4 x) + k_4 \dot{x} + k_5 x + k_6 \quad \text{(D-1)}$$

$$P_s = k_2 \ddot{x} + k_7 \dot{x} + k_8 x + k_9 \quad \text{(D-2)}$$

The solution of these equations, on the analog computer, is developed in this Appendix.

The variables in Eqs. (D1) and (D2) are non-dimensional in all respects except for time. For instance, the dimension of $\dot{x}^2$ as it appears in Eq. (D1) is sec^{-2}. Non-dimensionalization with respect to time is now advantageous for scaling purposes.

Letting non-dimensional time $\tau = \beta t$ and defining β such that

$$\beta^2 k_3 = 1 \quad \text{(D-3)}$$

we have, after substitution, elimination of P_s, and rearrangement

$$\ddot{x} = \frac{k_3}{k_2} \left[1 - (k_1 + k_6 + k_9) - \frac{k_2}{k_3} \ddot{x} (H_1 + H_2 x) - \dot{x}^2 (H_3 + H_4 x) - \beta (k_4 + k_7) \dot{x} \right] - \frac{k_3}{k_2} (k_5 + k_8) x \quad \text{(D-4)}$$

Note that although the notation has not been changed, all variables in Eq. (D-4) are completely non-dimensional. The expression for the acceleration has been written in the form of Eq. (D-4) in order

to illustrate the scheme of programming for the analog computer.

An auxiliary relation for the slug pressure P_s is

$$P_s = \frac{k_2}{k_3} \ddot{x} + k_7 \beta \dot{x} + k_8 x + k_9 \qquad \text{(D-5)}$$

The chamber pressure, P_c, can be developed by adding to P_s the pressure drops due to inertia and viscous effects in the chamber. The non-dimensional result is

$$P_c = P_s + T_1 + T_2$$

$$\text{where } T_1 = f_s \, x \, \dot{x}^2 \text{ and } T_2 = \frac{k_2}{k_3} \left(\frac{c}{m_s}\right) x \, \ddot{x} \qquad \text{(D-6)}$$

Equations (D-4) through (D-6) are shown in schematic form in Figs. D-1(a) and D-1(b). Figure D1(c) illustrates a modification necessary when the design is dominated by viscous effects (H_3>10) such as in the 5-inch baseline example of Section IV. It should be remarked that the logic of Fig. D-1 is based upon unit programming (reference voltage = 1 unit) and that the schematic illustrates the manner in which the equations were programmed for solution on two full-expanded EAI TR-20 10-volt analog computers. The primed component numbers in Fig. D-1(b) refer to the slaved computer and numbers without primes refer to components of the master unit. The table following Fig. D-1 lists the parameters determining the potentiometer settings in the analog program.

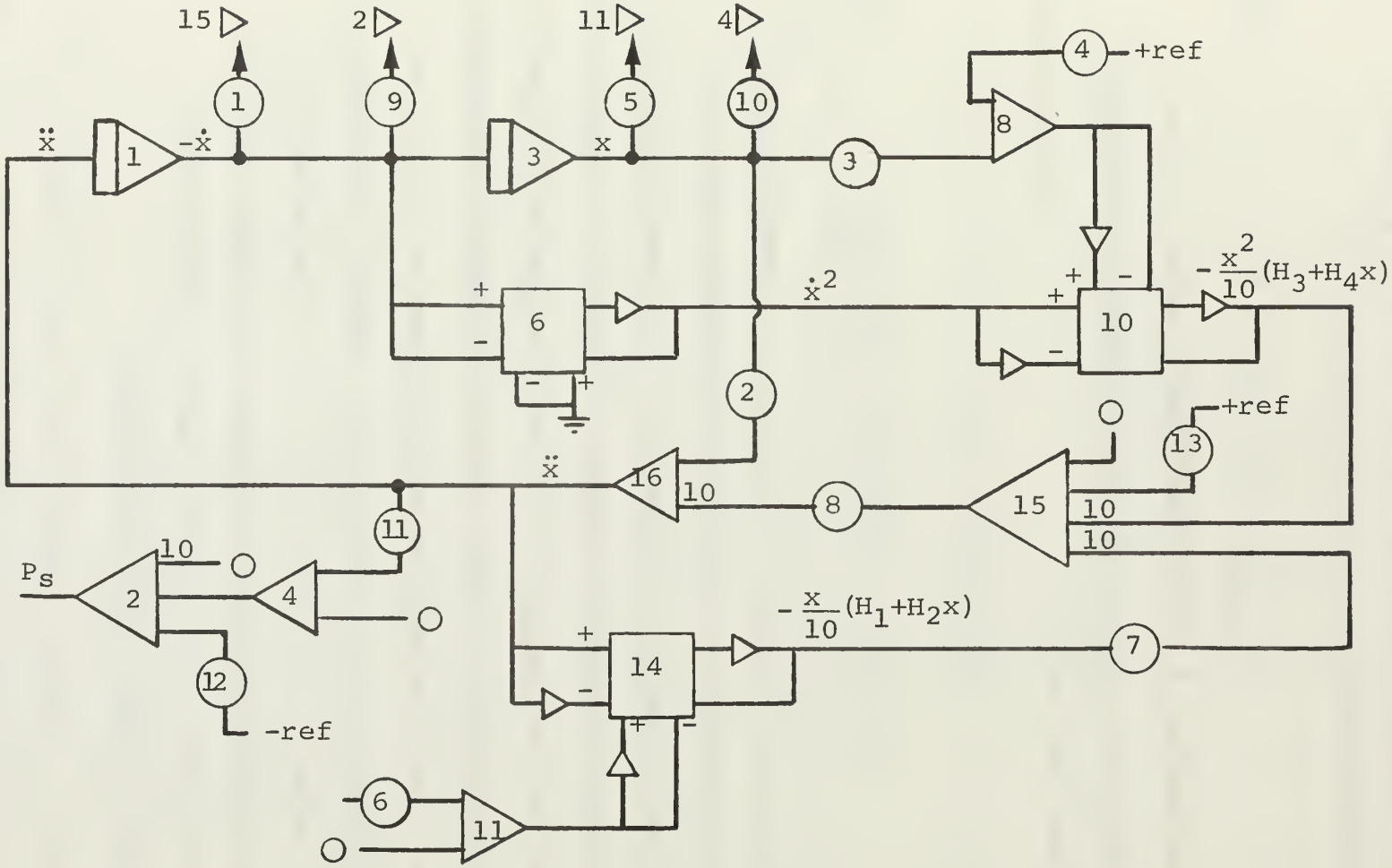

(a) Basic program, Eqs. (D4) and (D5).

Figure D1. Wiring schematic for analog solution.

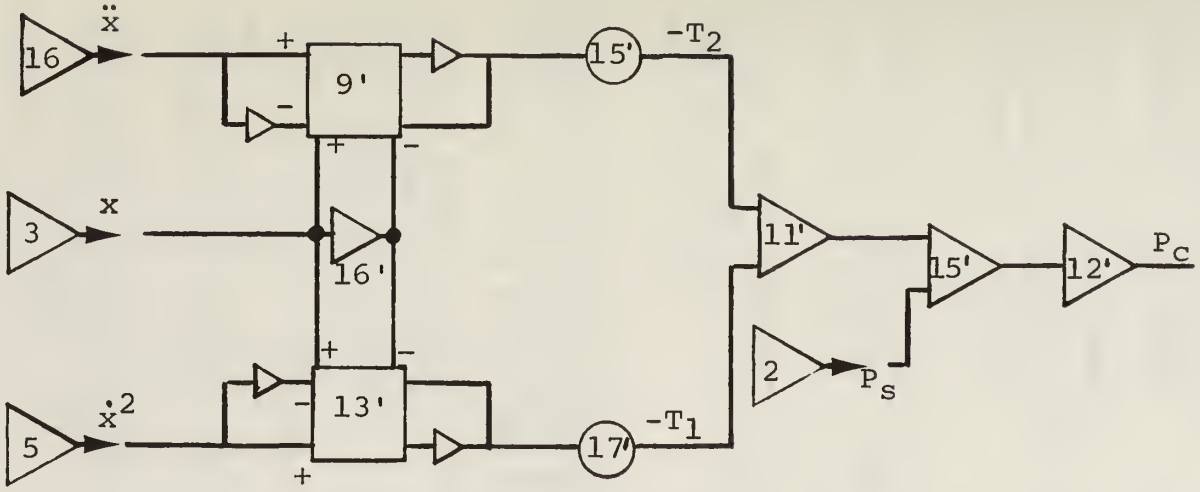

(b) Development of chamber pressure, P_c. Eq. (D6).

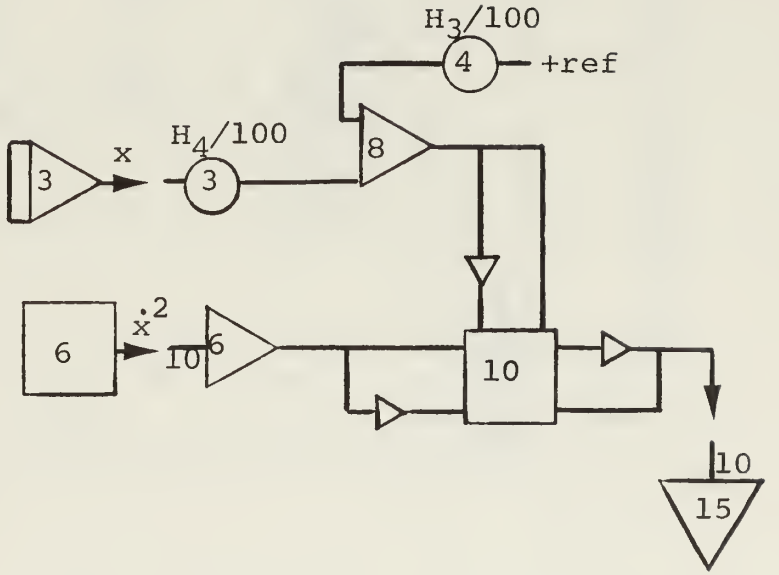

(c) Modification for large viscous effects.

Figure D1 (concluded).

Pot Number	Parameter
1	$(k_4 + k_7)\beta$
2	$(k_5 + k_8)\ (k_3/k_2)$
3	$H_4/10$
4	$H_3/10$
5	$H_2/10$
6	$H_1/10$
7	k_2/k_3
8	$k_3/10k_2$
9	$k_7\beta/10$
10	k_8
11	k_2/k_3
12	k_9
13	$1 - (k_1 + k_6 + k_9)$
15'	$(k_2/k_3)(c/m_s)$
17'	f_s

Table D-1. POT SETTINGS

INITIAL DISTRIBUTION LIST

Naval Ordnance Test Station 10
Attn: Code 5032E
Indian Head, MD 20640

Naval Sea Systems Command 5
Attn: NSEA 0331 (2)
CDR H. M. Effron, NSEA-65311 (1)
LCDR P. G. Rainey, NSEA-032 (1)
MAJ C. L. Carpenter, NSEA-03M (1)
Department of the Navy
Washington, D. C. 20362

Naval Air Systems Command 1
Attn: Mr. F. Marguardt, NAIR-350B
Department of the Navy
Washington, D. C. 20362

Naval Weapons Center 3
Attn: Mr. E. Romero, 4022 (2)
Mr. G. E. Kovalenko, 3053 (1)
China Lake, CA 93555

Defense Advanced Research Projects Agency 1
Attn: Mr. Charles Lehner (TTO)
1400 Wilson Blvd.
Rosslyn, VA 22209

Ballistics Research Laboratories 1
Aberdeen Research and Development Center
Attn: Mr. Richard Comer (AMXIBL)
Aberdeen Proving Ground, MD 21005

Chemical Propulsion Information Agency 1
Applied Physics Laboratory
Attn: Thomas W. Christian
8621 Georgia Avenue
Silver Spring, MD 20910

University of Utah 1
Attn: Dr. W. A. Guillory, Department of Chemistry
Salt Lake City, UT 84112

Naval Underwater Systems Center 2
Attn: Robert Heffernan (1)
G. E. Kovalenko (1)
Newport, RI 02840

R & D Associates
Attn: Dr. Ray Edelman
P.O. Box 3580
Santa Monica, CA 90403 — 1

University of California
Los Alamos Scientific Laboratory
Attn: Dr. Dan Butler (Code T-3)
P.O. Box 1663
Los Alamos, NM 87554 — 1

Pulsepower Systems, Inc.
Attn: Mr. L. Elmore
815 American St.
San Carlos, CA 93555 — 1

General Electric Co.
Armament Systems Dept.
Attn: E. Ashley
Burlington, VT 05401 — 1

General Electric Co.
Attn: Mr. J. Haskins (Rm. 1046)
100 Plastics Ave.
Pittsfield, MA 01201 — 1

Stanford Research Institute
Attn: Mr. G. A. Branch
333 Ravenswood Ave.
Menlo Park, CA 94025 — 1

Library
Naval Postgraduate School
Monterey, CA 93940 — 2

Dean of Research Administration
Naval Postgraduate School
Monterey, California 93940 — 2

Director
Defense Documentation Center
5010 Duke Street
Alexandria, Virginia 22314 — 12

Chairman, Department of Mechanical Engineering
Naval Postgraduate School
Monterey, California 93940 — 1

R. H. Nunn, Associate Professor of Mechanical Engineering
Naval Postgraduate School
Monterey, California 93940 — 10